Designing a Two-Echelon Distribution Network under Demand Uncertainty

Imen Ben Mohamed, Walid Klibi, François Vanderbeck

Designing a Two-Echelon Distribution Network under Demand Uncertainty

Imen Ben Mohamed[a,b,c,*], Walid Klibi[a,d], François Vanderbeck[b,c]

[a] *The Centre of Excellence in Supply Chain (CESIT), Kedge Business School, Bordeaux, France*
[b] *Mathematics Institute of Bordeaux (IMB), University of Bordeaux, Bordeaux, France*
[c] *RealOpt, Inria-Bordeaux-Sud-Ouest, Bordeaux, France*
[d] *Interuniversity Research Centre on Enterprise Networks, Logistics and Transportation (CIRRELT), Quebec, Canada*

Abstract

This paper proposes a comprehensive methodology for the stochastic multi-period two-echelon distribution network design problem (2E-DDP) where product flows to ship-to-points are directed from an upper layer of primary warehouses to distribution platforms (DPs) before being transported to the ship-to-points. A temporal hierarchy characterizes the design level dealing with DP location and capacity decisions, as well as the operational level involving transportation decisions as origin-destination flows. These design decisions must be calibrated to minimize the expected distribution cost associated with the two-echelon transportation schema on this network under stochastic demand. We consider a multi-period planning horizon where demand varies dynamically from one planning period to the next. Thus, the design of the two-echelon distribution network under uncertain customer demand gives rise to a complex multi-stage decisional problem. Given the strategic structure of the problem, we introduce alternative modeling approaches based on two-stage stochastic programming with recourse. We solve the resulting models using a Benders decomposition approach. The size of the scenario set is tuned using the sample average approximation (SAA) approach. Then, a scenario-based evaluation procedure is introduced to post-evaluate the design solutions obtained. We conduct extensive computational experiments based on several types of instances to validate the proposed models and assess the efficiency of the solution approaches. The evaluation of the quality of the stochastic solution underlines the impact of uncertainty in the two-echelon distribution network design problem (2E-DDP).

Keywords:
Supply chain management, Two-echelon Distribution Network Design, Location models, Uncertainty, Multi-period.

1. Introduction

The emergence of e-commerce and the arrival of innovative players, such as Amazon, have unquestionably changed the logistics landscape. More specifically, the major shift to an on-demand economy has tremendously affected the distribution schemas of several companies that aim to continue improving response time to customers while efficiently offering their products in a multi-channel setting. The delivery service level expectancy has significantly increased in the last decade: it is now expressed in hours rather than days. In addition, the ship-to-locations have recently evolved, making use of lockers, relay points, drives, and collection stores as alternatives to home delivery. In such context, several global B-to-C players, and retailers such as Walmart, Carrefour, Amazon or jd.com, have recently undertaken a sustained reengineering of their distribution networks. They have incorporated extra considerations to be closer to their key customer zones without reducing the efficiency of their consolidation policies in warehousing and transportation. For several global companies, the location of their primary warehouses followed various optimization rules going from centralization and risk-pooling incentives to sourcing-dependent and financial constraints. In practice, companies may have a single centralized

*Corresponding author
Email addresses: imen.benmohamed@kedgebs.com (Imen Ben Mohamed), walid.klibi@kedgebs.com (Walid Klibi), francois.vanderbeck@math.u-bordeaux.fr (François Vanderbeck)

warehouse or a reduced set of market-dedicated regional warehouses where they generally keep about a month or a season's worth of inventory depending on the demand dynamics and the production/sourcing cycles. When customers are globally deployed, these storage-locations are not specifically designed to provide next day and/or same day deliveries, especially when the customer bases are located in large geographic and almost urban areas. Such one-echelon networks constrain the companies' ability to provide fast delivery services, and reduce their opportunities to capture online orders.

In this new context, such strategic considerations imply a distribution schema with more than one-echelon that can be dynamically adjusted to the business needs over time. A typical predisposition schema, claimed now by practitioners, is the two-echelon distribution network. The network topology includes an intermediate echelon of distribution/fulfillment platforms located between the initial sites where inventory is held and the ship-to-points. For instance, Walmart plans to convert 12 Sam's Club stores into e-commerce fulfillment centers to support the rapid e-commerce growth [41]. City logistics is probably the most significant example of the shift from a one-echelon to a two-echelon distribution network setting [18, 50]. This is achieved by creating peripheral distribution/consolidation centers dedicated to transferring and consolidating freight from back-level platforms on large trucks into smaller and environmentally friendly vehicles, more suitable for city distribution. Parcel delivery is also a relevant context where two-echelon distribution networks operate [30]. With this in mind, most of the literature considers the one-echelon network topology to characterize distribution operations where the aim is to find optimal locations, minimize the number of depots, and build routes around the depots to serve customers [54]. At the tactical level, the notion of multi-echelon distribution is well studied from an inventory optimization perspective [31], however, its strategic counterpart is less developed [22, 19]. Several authors have recently recalled the need to expand one-echelon networks by considering an intermediate echelon of platforms where storing, merging, consolidation or transshipment operations take place [12].

This is specifically the focus of this paper where we address the two-echelon distribution-network design problem (2E-DDP). This strategic problem aims to decide on the number and location of distribution platforms (DPs), and the capacity allocated to these platforms to efficiently distribute goods to customer ship-to-bases. It also integrates the allocation decisions related to the assignment of ship-to-points to DPs, and DPs to primary warehouses. The overriding challenge of a two-echelon setting is that the location of such DPs does not only depend on the trade-off between ship-to-point demand versus DP capacity and the type of outbound routes that could be designed, but is also influenced by the inbound assignment/replenishment policy and the trade-off between location versus capacity at the preceding echelon. Furthermore, in view of the demand process, the cost variability over time, and demand uncertainty, the question is when and how much distribution capacity to add to the network. We address this related issue by examining the periodic capacity decisions for the distribution network over a multi-period planning horizon. Figure 1 illustrates a typical 2E-DDP where the network is partitioned into two capacitated distribution echelons. Each echelon has its own assignment-transportation schema that must be adapted in response to the uncertainty shaping the business horizon.

Some authors consider such a distribution context by explicitly modeling routes to formulate the two-echelon location-routing problem (2E-LRP) as an extension of the well-known location-routing problem (LRP) [46]. The 2E-LRP is formally introduced in Boccia et al. [12] in an urban context and is further studied by Contardo et al. [15]. However, the literature on 2E-LRP is still scarce and considers only a deterministic-static setting [54, 22, 19]. Additionally, 2E-LRP and most LRP modeling approaches implicitly assume that location and routing decisions are made simultaneously for the planning horizon, without considering the hierarchical structure of the strategic problem stressed here. Alternatively, some papers use a hierarchical approach to the two-echelon distribution problem, extending the facility location problem (FLP) [33, 21], to the two-echelon facility location problem (2E-FLP) introduced in [28]. However, most 2E-FLP studies approximate the transportation and fulfillment characteristics related to the distribution case, ignoring the capacity decisions, and studying mostly deterministic versions. Furthermore, we note that most production-distribution problems have implicitly a two-echelon structure, but with a single distribution echelon. They are relying on FLP formulation and focusing on functional expansions related to production policies/constraints, and specific manufacturing-linked transportation issues, rather than the strategic needs of the distribution stressed above (see for instance [67, 6, 7, 27]). Comprehensive reviews on FLPs can be found in [49, 26].

Moreover, given the strategic nature of decisions in 2E-DDP, the network must be designed to last for

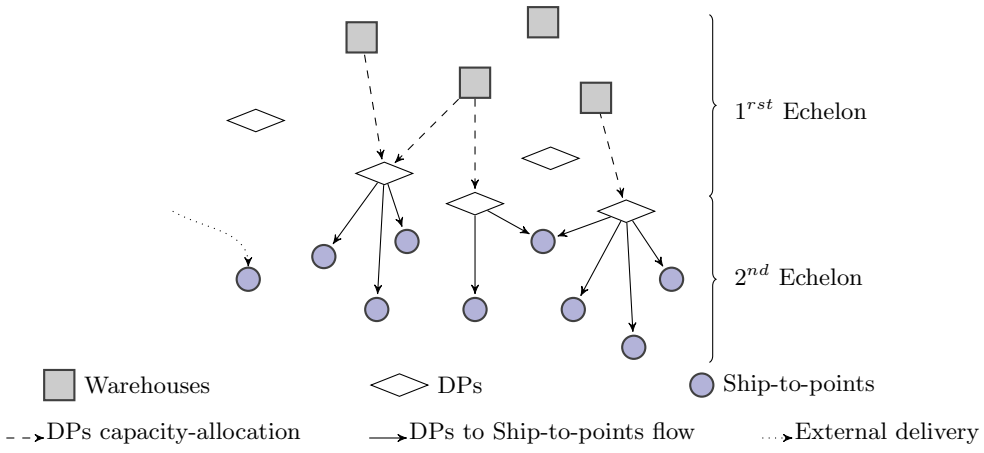

Figure 1: A potential Two-Echelon Distribution Network Design Problem (2E-DDP)

several years, fulfilling future requirements and be efficiently adaptable to changes in the business environment over time. According to the Tompkins report in (2011) [14], there is a significant trend in practice toward reducing the planning horizon in strategic studies from 4 years to under 2 years due to business uncertainty and complexity. Accordingly, the traditional deterministic-static representation of the planning horizon must be replaced by a more realistic stochastic-multi-period characterization of the planning horizon. More specifically, the horizon is modeled with a set of planning periods shaping the evolution/uncertainty of random factors (e.g., demand, costs, etc.), and promoting the structural adaptability of the distribution network. Such decisional framework leads to a multi-stage stochastic programming problem as addressed here. Despite the fact that the multi-stage stochastic programming framework is well established [61, 11], its application to distribution problems is still in its infancy. Recently, some authors [52, 44, 23] raise the need for such a decisional framework to tackle complex supply chain problems.

The aim of this paper is thus to first define 2E-DDP under uncertain and time-varying demand, and time-varying DP opening costs, formulated as a multi-stage stochastic program with recourse. Our modeling framework considers that the planning horizon is composed of a set of planning periods shaping the evolution of uncertain ship-to-point demand over time. It also assumes that the number and location of DPs are not fixed a priori and must be decided at the strategic level along the set of planning periods. Furthermore, it considers strategic assignment-transportation decisions to calibrate DP throughput capacity based on transportation capabilities. Our approach looks at a hierarchical strategic-operational decisional framework where the emphasis is on the network design decisions and their impact on the company's distribution performance. The operational decisions related to transportation operations are modeled as origin-destination flows, which correspond to a sufficiently precise aggregate of daily decisions over several products, transportation means, and working periods, as discussed in [45]. Second, 2E-DDP is an NP-hard stochastic combinatorial optimization problem since it inherits several complexities from the FLP and LRP models, in addition to the curse of dimensionality of its multi-stage stochastic setting. This justifies the development of approximate modeling approaches that allow handling realistic instances and guarantee the generation of good-quality design solutions. Consequently, we propose solvable two-stage stochastic versions of the 2E-DDP. These models differ in the modeling of distribution operations, and we discuss their solvability with respect to the capabilities of current solvers. Our solution methodology builds on a Benders decomposition [10] and on the sample average approximation (SAA) method [61] to formulate the deterministic equivalent model with an adequate sample size of scenarios. The results obtained from the extensive experiments show the trade-off between solvability and the quality of the designs produced by both models. They also illustrate the importance of tackling the stochastic problem by evaluating the quality of the stochastic solutions. Several managerial insights are also derived on the behavior of design decisions under the stochastic-multi-period characterization of the planning horizon.

The remainder of this paper is organized as follows. Section 2 summarizes the related works on distribution

network design models under deterministic and stochastic settings, and the exact solution methods applied to such models. Section 3 defines the 2E-DDP, presents the characterization of the uncertainty by scenarios, and provides a comprehensive multi-stage stochastic formulation. Section 4 discusses the solvability of our model and introduces two-stage stochastic program approximations of the multi-stage model that make it tractable. Section 5 presents the solution approaches proposed to solve the problem using Benders decomposition and the SAA technique. It also introduces an evaluation procedure to assess the quality of the stochastic solutions, and evaluate the performance of the designs obtained. Section 6 reports our computational results and discusses the quality of the solutions obtained in conjunction with the solvability effort of the associated models. Section 7 provides conclusions and outlines future research avenues.

2. Related works

2E-DDP is closely related to several classes of problems in the operations research (OR) literature that we classify according to their modeling options. Table 1 presents the main studies related to 2E-DDP and classifies the related works in terms of network structure (the echelons involved in the network other than the ship-to-point level), and provides the main distinguishing features in terms of the distribution operations (routes (R) versus flows (F)) and capacity planning decisions under single/multi-period (SP vs MP) and deterministic (D)/stochastic (S) settings. Table 1 also highlights the mathematical modeling and the solution approaches used to tackle the problem.

As mentioned in Table 1, existing studies include different numbers and types of echelons. The echelons differ in terms of location decisions as an implicit or explicit decision. Boccia et al. [12] and Sterle [65] formulate a static two-echelon distribution problem as a 2E-LRP where location decisions involve warehouses and distribution centers, and distribution operations are modeled by routes. They introduce a two-index and three-index vehicle-flow formulation, and a set-partitioning formulation. Nguyen et al. [50, 51] study a special case of 2E-LRP in the urban context including one single main warehouse at the first echelon and several potential distribution centers. Correia et al. [16] focus on a multi-period two-echelon network with central and regional distribution centers where distribution decisions are approximated by flows. Supply chain networks have provided suitable applications of FLPs in the last decades. Ambrosino and Scutellà [5] and Georgiadis et al. [29] address designing a supply chain network comprising a two-echelon distribution schema in addition to inbound flows (i.e., from suppliers/plants). Further studies use the two-echelon structure in supply chain network design problems [17, 27, 70], in closed loop supply chains [69], and in production-distribution problems [13, 67], but only considering a single distribution echelon. These studies are oriented toward functional expansions, such as production policies and constraints, and specific manufacturing-linked transportation issues, rather than focusing on the strategic needs of the distribution businesses. In this study, we assume that the two echelons are dedicated to distribution operations, i.e., responsible for the delivery of finished goods (see for instance [16, 29]).

The complexities of distribution systems in real world applications lead to integrating operational decisions at the strategic level. More specifically, capacity decisions as strategic/design planning decisions and transportation and distribution policies as operational planning decisions are included in 2E-DDPs, as well as classic location-allocation decisions. Moreover, considering a time horizon of multiple periods is of great importance to decision-makers, since facility location decisions are long-term problems. Ambrosino and Scutellà [5], Georgiadis et al. [29] and Heckmann et al. [34] limit the multi-period settings to operational decisions, and the strategic decisions are taken once at the beginning of the planning horizon, whereas Correia et al. [16] and Darvish et al. [20] consider multi-period settings for strategic decisions. In [43], a single design period is used and coupled with multiple operational periods. Albareda-Sambola et al. [4] tackle a multi-period LRP where two interconnected time scales for design and operational decisions are considered.

In addition, considering multiple design periods enables making adjustments to location decisions through opening (O), closing (C), and/or reopening (Re) facilities [52, 20, 53], and adjustments to facility capacities through reduction and expansion [16, 1, 70] in each design period due to demand variability over time (see Table 1). Pimentel et al. [53] focus on the one-echelon stochastic capacity planning and dynamic network design problem in which warehouses can be opened, closed, and reopened more than once during a planning horizon. This is more suited to new warehouses that are being rented instead of built, since lower fixed setup

costs are incurred. Heckmann et al. [34] introduce a single echelon risk-aware FLP in which capacity expansions with different levels are possible in each facility and the risk is evaluated through customer satisfaction. Capacity expansion are declared as first-stage decision and the selection of the type of expansion level for every period is depicted as second-stage decision. Jena et al. [40] introduce the one-echelon dynamic facility location problem with generalized modular capacities that generalizes existing formulations for the multi-period FLP: the problem with facility closing and reopening, the problem with capacity expansion and reduction, and their combination.

One-echelon distribution problems under uncertainty are studied in the literature in [57, 34] and [59] where stochasticity is assumed for demand and facility capacities. Additionally, incorporating a multi-period planning horizon with uncertainty is investigated in Aghezzaf [1], and Zhuge et al. [70] in the supply chain context with one distribution echelon to meet the variability of demand uncertainty. Zhuge et al. [70] also consider an uncertain and time varying budget. Georgiadis et al. [29] combine multiple operational periods with the stochastic setting in a two-echelon distribution configuration where product demand is uncertain and time varying.

In the 2E-DDP, distribution operations may take the form of routes (R) or direct flows (F) generalizing the classic problems in the literature: 2E-LRPs [19] and 2E-FLPs [49, 26], respectively. Table 1 shows that the majority of papers using routes are studied in a deterministic-static setting, and to the best of our knowledge, no work has yet addressed the multi-period and stochastic settings simultaneously. However, some papers consider the multi-period and stochastic settings in 2E-FLPs and supply chain network design, but its application to the two-echelon distribution configuration is still limited.

Furthermore, Table 1 shows that most studies in the deterministic-static and multi-period setting are formulated with a mixed-integer linear program (MILP)(for instance, [15, 16]). Nevertheless, under uncertainty, stochastic programming approaches are more appropriate as in [29, 34, 70], where the problem is modeled as a mixed-integer two-stage stochastic program with recourse (TSSP). Integrating a multi-period setting with uncertainty in long-term problems leads to multi-stage stochastic programming (MSSP) [36]. This approach is applied in Nickel et al. [52], Albareda-Sambola et al. [3], and Pimentel et al. [53] for the one-echelon distribution network, and in Zeballos et al. [69] for the closed-loop supply chain context. Ahmed et al. [2] formulate the multi-period capacity expansion problem as a MSSP where both the demand and investment costs are uncertain.

The multi-stage modeling approach adds complexity to the problems. Theoretical developments and approximations are proposed in the literature: Guan et al. [32] present cutting planes for multi-stage stochastic integer programming enhanced by inequalities that are valid for individual scenarios. When a set of scenarios is assumed for modeling uncertainty in a multi-stage setting, it is possible to build a scenario tree. However, in practice, accurate approximations of a complex stochastic process with a modest-sized scenario tree represent a very difficult problem. Thus, several scenario generation methods and reduction techniques are proposed. We refer the reader to Heitsch and Römisch [35], Dupačová et al. [24, 25], and Høyland and Wallace [37]. Römisch and Schultz in [56] explore the scenario tree and propose a path-based alternative modeling framework. Later, Huang and Ahmed [38] used the same framework to improve the modeling of uncertainties in a MSSP context.

Accordingly, no work addresses the multi-stage stochastic framework for the multi-period stochastic 2E-DDP. Furthermore, although some works propose tackling mixed-integer multi-stage stochastic programs using exact and heuristic methods based on decomposition techniques and/or scenario sampling methods [58, 11], further progress is required to solve realistic two-echelon distribution design problems.

Table 1: Network structure, key decisions and solution approaches in multi-period planning horizon distribution network studies

Article	**Network structure**			**SP/MP**	**D/S**	**Distribution operations**	**Capacity Planning**	**Location status per time period**	**Mathematical modeling**	**Solution approach**
	S/P	W	DC							
Jacobsen and Madsen [39]	-		√	SP	D	R	*Fc*	1—O		Three constructive heuristics
Boccia et al. [12]		√	√	SP	D	R	*Fc*	1—O	Three MILPs	Commercial solver
Nguyen et al. [50]		-	√	SP	D	R	*Fc*	1—O	ILP	GRASP
Nguyen et al. [51]		-	√	SP	D	R	*Fc*	1—O	MILP	MS-ILS
Contardo et al. [15]		√	√	SP	D	R	*Fc*	1—O	MILP	Branch-and-Cut and ALNS
Darvish et al. [20]		-	√	MP	D	R	*Fc*	T—O	MILP	Commercial solver + valid inequalities
Ambrosino and Scutellà [5]	-	√	√	MP	D	R	*Fc*	1—O	MILP	Lagrangean-based heuristic
Correia et al. [16]		√	√	MP	D	F	*Dv*	T—O	MILP	Commercial solver
Georgiadis et al. [29]	-	√	√	MP	S	F	*Dv*	1—O	TSSP	Commercial solver
Heckmann et al. [34]		√		MP	S	F	*Dv*	1—O	TSSP	Commercial solver
Aghezzaf [1]	-	√		MP	S	F	*Dv*	T—O	Robust model	Lagrangian relaxation decomposition
Zhuge et al. [70]	-		√	MP	S	F	*Dv*	T—O	TSSP	Lagrangian-based heuristic
Albareda-Sambola et al. [3]		√		MP	S	F	*U*	T—O/C	MSSP-and-TSSP	Fix-and-Relax-Coordination algorithm
Nickel et al. [52]			√	MP	S	F	*Fc*	T—O	MSSP	Commercial solver
Pimentel et al. [53]		√		MP	S	F	*Dv*	T—O/C/Re	MSSP	Lagrangian-based heuristic
Zeballos et al. [69]	√	√	√	MP	S	F	*Fc*	T—O/C	MSSP	Commercial solver
Our work		-	√	MP	S	F	*Dv*	T—O/C/Re	MSSP-and-TSSP	Benders decomposition+SAA

S/P: Supplier/Plant, W: Warehouse, DC: Distribution center.

-: Implicit decision, √ : Explicit decision.

U: Uncapacitated, *Fc*: Fixed capacity a priori, *Dv*: Decision variable.

O: Opening new locations, C: Closing existing locations, Re: Reopening closed locations.

The aforementioned studies mostly use commercial solvers to solve their mathematical programs as in [16, 29, 12]. Exact solution methods are proposed to solve the two-echelon distribution configuration, such as the branch-and-cut algorithm in [15]. Lagrangian-based heuristics in [5] are the most popular heuristics used in this context. Metaheuristics are also proposed to solve the deterministic and static 2E-DDP with routes such as the Greedy Randomized Adaptive Search Procedure (GRASP) in [50], the Multi-Start Iterated Local Search (MS-ILS) in [51], and the Adaptive Large Neighborhood Search (ALNS) [15]. Sampling methods [60] such as sample average approximation (SAA) are used in stochastic models to limit the large number of scenarios. This is applied in supply chain network design problems with a one distribution echelon in [57, 68, 59, 43]. Santoso et al. [57] integrate the SAA scheme with an accelerated Benders decomposition algorithm to quickly compute high quality solutions to large-scale stochastic supply chain design problems with a vast number of scenarios.

3. The two-echelon multi-period distribution network design problem

3.1. Problem definition

We consider the business context of a retail company that sources a range of products from a number of supply sites (e.g., suppliers, manufacturing plants), and stores them at primary warehouses. Without loss of generality, these products are aggregated in a single product family in our modeling approach because they are relatively uniform and share the same handling and storage technology [48]. This is done by taking average cost and demand information related to the entire product family. Under a make-to-stock policy, the company operates a set of primary warehouses, formerly designed to centralize inventories and ensure distribution to demand zones periodically. However, the locations of the company warehouses are not necessarily designed to provide next day and/or same day delivery. To do so, the company needs to deploy an advanced set of distribution resources to serve ship-to-points with an adequate service level. Strategic facility-location decisions concern a new intermediate echelon, dimensioning capacitated DPs used to fulfill orders and deliver finished goods to ship-to-points. This 2E-DDP is illustrated in Figure 1: strategic decisions concern the location of DPs at the intermediate level and the capacity of the links between the warehouses and the ship-to-locations.

Ship-to-point orders vary in quantity of product demanded on a daily basis. Once a given set of DPs is deployed, the company periodically determines the quantity of goods to be allocated to each DP: this translates into a number of full-load trucks required from warehouses to deliver products to a DP. Then, on a daily basis, the goods are delivered to ship-to-locations through common or contract carriers for each single ship-to-point. Thus, while the allocation decisions are modeled as periodic origin-destination quantities from warehouses to DPs, the transportation decisions are modeled as daily transportation links from DPs to ship-to-points. Our focus is on strategic capacity allocation decisions made by distribution platforms and their transportation capabilities. The operational shipping decisions are modeled to capture the running cost of strategic decisions. To ensure feasibility, a recourse delivery option is allowed if the ship-to-points cannot be satisfied from the set of deployed DPs on a given day. This recourse comes at a higher shipment cost. Our model considers a long-term planning horizon $\mathcal{T}$ that covers a set of successive design planning periods $\mathcal{T} = \{1, \ldots, T\}$. Such periods are defined in accordance with the operational dynamics such that a planning period corresponds to a year, which is typical in the context of DPs to lease. Each planning period covers a set of operational periods, represented generally in a discrete way by "typical" business days. Figure 2 illustrates the relationship between the decision planning periods and operational days, and the hierarchical structure of the decision problem. It also shows that strategic design decisions (location and capacity decisions) could be adapted periodically at each design period t to align the distribution network to its business environment, especially when operating under uncertainty. Worth noting is that the design decisions must be made prior to their deployment period with partial information on the future business environment. After an implementation period, they will be available for use as shown by the positioning of the arrows in Figure 2. This assumes information asymmetry between the design level and the operational level, mainly due to the fact that the decisions are not made at the same time. Therefore, our model has a multi-stage decision structure. At the beginning of the planning horizon, the here and now design decisions are made, and are thus considered as the first-stage DP design decisions. Next, at the beginning of each subsequent period ($t > 1$), a new opportunity to adapt the distribution network structure to its future environment is offered, based on the information available at that time. Decisions made

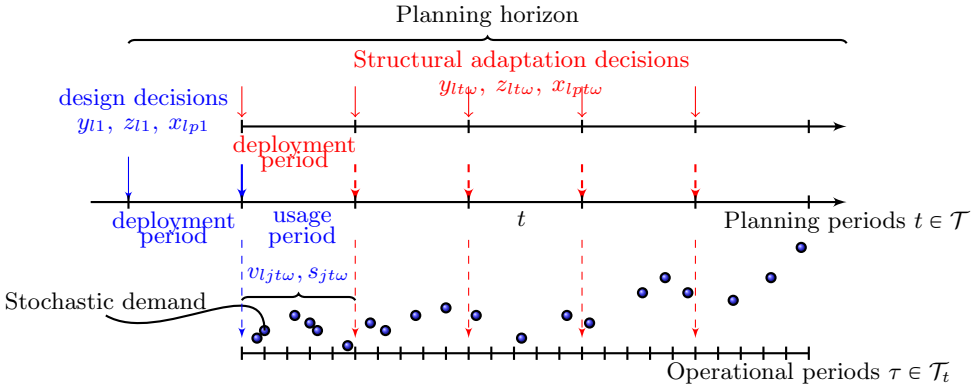

Figure 2: Decision time hierarchy for the planning horizon under uncertainty

at the beginning of the period t depend on the design decisions up to that period, as illustrated in Figure 2 and described mathematically in the stochastic 2E-DDP model below.

3.2. Scenario building and tree representation

Uncertain daily demand of ship-to-points is represented by a random variable, which is estimated by a given probability distribution. Let d_j be the random variable for ship-to-point j demand that follows a distribution probability F_j with a mean value μ_{j0} estimated from historical data until $t = 0$. Under a multi-period planning horizon setting, the random demand process is time-varying. More specifically, a multi-period plausible future allows capturing factor transitions (inflation-deflation, population density, ~~market stores,~~ etc.) that perturb the a priori estimation of demand behavior and could thus impact the design decisions. This means that a trend function is associated with the random variable and the associated distribution probability F_{jt} with a mean value μ_{jt} to shape demand realization.

The uncertainty is characterized by a set Ω of plausible future scenarios where a scenario ω encompasses the demand realization for each period t and for all the ship-to-points during a typical business day. Then, at the beginning of each period t, the information available is updated according to the additional data revealed up to t. Let Ω_t be the subset of distinct scenarios of Ω that share the same realization up to stage t. Hence, $\Omega_T = \Omega$. Thus, $d_{jt\omega}$ will denote the demand of ship-to-point j at period t under scenario $\omega \in \Omega_t$ following the distribution probability F_{jt} with the parameters μ_{jt}. Given the entire planning horizon, a scenario tree $\mathscr{T}$ should be built to characterize the realization of demand for each planning period. When using such stochastic process, scenario instances can be generated with Monte Carlo methods. At each stage t, a discrete number of nodes represent points in time where realizations of the uncertain parameters take place and decisions have to be made. Each node g of the scenario tree, except the root, is connected to a unique node at stage $t-1$, called the ancestor node $a(g)$, and to nodes at stage $t+1$, called the successors. We denote with $\pi_{a(g),g}$ the conditional probability of the random process in node g given its history up to the ancestor node $a(g)$. The path from the root node to a terminal (leaf) node corresponds to a scenario ω, and represents a joint realization of the problem parameters over all periods $1, \ldots, T$. Partial paths from the root node to intermediate nodes correspond to the restricted scenarios up to stage t denoted ω^t.

Figure 3(a) illustrates a typical multi-stage scenario tree. The scenario probability is obtained by multiplying the conditional probabilities through the path. The non-anticipativity principle [55] is implemented by requiring that the decisions related to scenarios that are identical up to a given stage are the same and can therefore be represented by a single variable. In the following, we use branches of the scenario tree to define recourse variables where each branch represents a restricted scenario $\omega^t \in \Omega_t$ [24]. Accordingly, using restricted scenarios, one can avoid to write the non-anticipativity constraints explicitly. Further, we should point out that an alternative node-based formulation is presented by Beltran-Royo et al. [8] and used in some studies as in [3, 53]. This latter is based on the scenario tree nodes to formulate the multi-stage stochastic program.

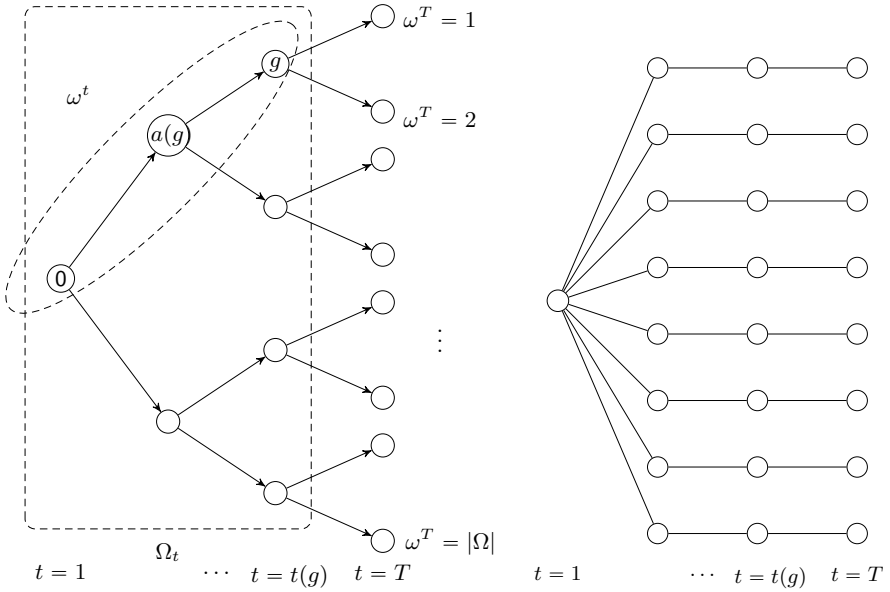

(a) Multi-stage scenario tree (b) Fan of individual scenarios

Figure 3: Scenario tree representation and notations

3.3. The multi-stage stochastic formulation

The stochastic 2E-DDP can be modeled as a multi-stage stochastic program with a set of scenarios. As mentioned above, Ω_t represents the set of distinct restricted scenarios up to stage t, for all $t = 1, \ldots, T$: $\Omega_t = \{\omega^t : \omega \in \Omega\}$. For the sake of simplification, we use $\omega \in \Omega_t$ when modeling the problem. We also consider the following notations:

- Sets

  $prec(\omega)$ the set of direct ancestors of scenario $\omega \in \Omega_t$, for all $t = 1, \ldots, T-1$: $prec(\omega) = \{\omega' \in \Omega_{t-1} : \omega_\tau(\omega) = \omega_\tau(\omega'), \forall \tau < t\}$.

  $\mathcal{P}$ set of primary warehouses.

  $\mathcal{L}$ set of distribution platforms (DPs).

  $\mathcal{J}$ set of ship-to-points.

- Parameters

  $p(\omega)$ the probability of each scenario $\omega \in \Omega_t$. Note that $\sum_{\omega \in \Omega_t} p(\omega) = 1$ for all t.

  C_p is the maximum throughput capacity of primary warehouse $p \in \mathcal{P}$ (expressed in flow unit for a given period).

  C_l is the maximum capacity of the DP $l \in \mathcal{L}$.

  C_{lp} is the maximum capacity of transportation used for flows from warehouse $p \in \mathcal{P}$ to DP $l \in \mathcal{L}$.

  c_{ljt} is the transportation cost per product unit from a DP $l \in \mathcal{L}$ to ship-to-point $j \in \mathcal{J}$ at period $t \in \mathcal{T}$.

  c_{lpt} is the unit transportation cost per flow unit from warehouse $p \in \mathcal{P}$ to DP $l \in \mathcal{L}$ at period $t \in \mathcal{T}$.

  f^s_{lt} is the cost of opening a DP $l \in \mathcal{L}$ at period $t \in \mathcal{T}$.

  f^u_{lt} is the cost of operating a DP $l \in \mathcal{L}$ at period $t \in \mathcal{T}$.

  c_{jt} is the shipment cost when recourse delivery is employed to cover a proportion of the demand of a ship-to-point $j \in \mathcal{J}$ at period $t \in \mathcal{T}$.

Note that since transportation decisions are made for a typical business day, the operational transportation costs c_{ljt} and c_{jt} are annualized to adequately cover the horizon length in the objective function.
The decision variables are:

$z_{lt\omega} = 1$ if DP $l \in \mathcal{L}$ is opened under scenario $\omega \in \Omega_t$, $t = 1, \ldots, T$, 0 otherwise.

$y_{lt\omega} = 1$ if DP $l \in \mathcal{L}$ is operating under scenario $\omega \in \Omega_t$, $t = 1, \ldots, T$, 0 otherwise.

$x_{lpt\omega}$ = Inbound allocation from warehouse $p \in \mathcal{P}$ to DP $l \in \mathcal{L}$ expressed in number of truckload units contracted to deliver from the warehouse under scenario $\omega \in \Omega_t$, $t = 1, \ldots, T$.

$v_{ljt\omega}$ = fraction of demand delivered from DP $l \in \mathcal{L}$ to ship-to-point $j \in \mathcal{J}$ under scenario $\omega \in \Omega_t$, $t = 1, \ldots, T$.

$s_{jt\omega}$ = fraction of demand of ship-to-point $j \in \mathcal{J}$ satisfied from a recourse delivery under scenario $\omega \in \Omega_t$, $t = 1, \ldots, T$ (i.e., external shipment, not from DPs).

The deterministic equivalent formulation for the multi-stage stochastic problem takes the form:

$$\text{(MS-M)}\min \sum_{t\in\mathcal{T}}\sum_{\omega\in\Omega_t} p(\omega)\Big(\sum_{l\in\mathcal{L}}\big[(f^u_{lt}\, y_{lt\omega} + f^s_{lt}\, z_{lt\omega}) + \sum_{p\in\mathcal{P}} c_{lpt}\, C_{lp} x_{lpt\omega}\big] + \sum_{j\in\mathcal{J}} d_{jt\omega}\big[\sum_{l\in\mathcal{L}} c_{ljt}\, v_{ljt\omega} + c_{jt}\, s_{jt\omega}\big]\Big) \tag{1}$$

$$\text{S. t.} \quad \sum_{l\in\mathcal{L}} C_{lp} x_{lpt\omega} \leqslant C_p \qquad \forall p \in \mathcal{P}, t \in \mathcal{T}, \omega \in \Omega_t \tag{2}$$

$$\sum_{p\in\mathcal{P}} C_{lp} x_{lpt\omega} \leqslant C_l y_{lt\omega} \qquad \forall l \in \mathcal{L}, t \in \mathcal{T}, \omega \in \Omega_t \tag{3}$$

$$y_{lt\omega} - y_{ltprec(\omega)} \leqslant z_{lt\omega} \qquad \forall l \in \mathcal{L}, t \in \mathcal{T}, \omega \in \Omega_t \tag{4}$$

$$\sum_{j\in\mathcal{J}} d_{jt\omega}\, v_{ljt\omega} \leqslant \sum_{p\in\mathcal{P}} C_{lp} x_{lpt\omega} \qquad \forall l \in \mathcal{L}, t \in \mathcal{T}, \omega \in \Omega_t \tag{5}$$

$$\sum_{l\in\mathcal{L}} v_{jlt\omega} + s_{jt\omega} = 1 \qquad \forall j \in \mathcal{J}, t \in \mathcal{T}, \omega \in \Omega_t \tag{6}$$

$$x_{lpt\omega} \in \mathbb{N} \qquad \forall l \in \mathcal{L}, p \in \mathcal{P}, t \in \mathcal{T}, \omega \in \Omega_t \tag{7}$$

$$y_{lt\omega}, z_{lt\omega} \in \{0, 1\} \qquad \forall l \in \mathcal{L}, t \in \mathcal{T}, \omega \in \Omega_t \tag{8}$$

$$v_{ljt\omega} \geqslant 0 \qquad \forall l \in \mathcal{L}, j \in \mathcal{J}, t \in \mathcal{T}, \omega \in \Omega_t \tag{9}$$

$$s_{jt\omega} \geqslant 0 \qquad \forall j \in \mathcal{J}, t \in \mathcal{T}, \omega \in \Omega_t \tag{10}$$

The objective function (1) seeks to minimize the total expected cost for the design and operational costs throughout the planning horizon. The first and second terms refer to the design costs that include the operating and opening costs for DPs, and the inbound allocation cost to DPs from warehouses. The third term represents the transportation cost in the second echelon (from DPs to ship-to-points) as well as the external delivery costs. Constraints (2)-(3) express capacity limit on warehouses and DPs, respectively, over stages. In addition, constraints (3) force that a delivery is possible to a DP only if it is operating. Constraints (4) define the setup of the DPs over stages. These constraints manage the status of the DPs operating from one stage to the next and set their opening. Constraints (5) aim to cover the demand of ship-to-points from the operating DPs without exceeding their inbound allocation from warehouses. Constraints (6) ensure that a ship-to-point is either satisfied through the opened set of DPs or through a recourse delivery. All the other constraints (7)-(10) define the decision variables of the problem. Observe that $|\Omega_1| = 1$ and therefore decisions (x, y, z) at the first stage represent here and now decisions concerning the design. Their counterpart at later periods represents recourse on the design in this multi-stage process. On the other hand, allocation decisions (v, s) allow evaluating the operational cost of the distribution system given design (x, y, z) that is fixed in each period.

4. Two-stage stochastic program approximations

The above multi-stage stochastic formulation of the 2E-DDP highlights the hierarchical structure of the problem and the scenario-based relation between the different decisions. For realistic size problems, explicitly tackling such multi-stage stochastic programs using exact and heuristic methods is beyond the scope of current

technologies [58, 11]. We build here on the reduction [42, 63] and relaxation [62] approaches recently applied to transform the multi-stage stochastic program to a two-stage stochastic program, and transform the multi-stage stochastic program (1)-(10) into a two-stage stochastic program that is sufficiently accurate to capture the essence of the problem while being solvable in practice.

Accordingly, one modeling approach consists in transferring from the MS-M model all the design decisions of the T periods (location and capacity-allocation) to the first-stage in order to be set at the beginning of the horizon. In this case, only first-stage design decisions ($t = 1$) are made here and now, but subsequent design decisions ($t > 1$) (see Figure 2) are essentially used as an evaluation mechanism. These latter design decisions for periods ($t > 1$) are deferrable in time according to their deployment period. Therefore, the obtained model offers an approach to set the design decisions for ($t = 1$) with an optimistic evaluation at the beginning of the horizon of subsequent design decisions without losing its hedging capabilities. This approach gives rise to the two-stage stochastic location capacity-allocation model. This model is challenging to solve due to the combinatorial difficulty of its mixed-integer program and the high number of scenarios. Another modeling approach consists in transferring from the MS-M only the T periods' design decisions related to the location decisions to the first-stage, and relaxing the capacity-allocation decisions to the second-stage for all periods. These latter capacity-allocation decisions now become part of the recourse problem and thus scenario-dependent (see Figure 2). This approach gives rise to the two-stage stochastic flow-based location-allocation model.

The discussion above impacts the scenario building approach: for stages $t \geqslant 2$, the scenario tree construction algorithm can reduce the number of nodes to a fan of individual scenarios that prescribes the random parameter value for the full time horizon with a probability $p(\omega), \omega \in \Omega_t$. This is illustrated in Figure 3(b) where scenarios are independent of the number of periods, as discussed in [24]. Thus, the scenario representation fan of the planning horizon fits well with our two-stage stochastic programming and clearly simplifies the generation of scenarios. The rest of the section provides the formulation of these two design models for the 2E-DDP.

4.1. Location and capacity-allocation model (LCA)

In this two-stage model, the design decisions for ($t > 1$) can be taken at the beginning of the planning horizon and do not depend on the history up to period t. In this case, the first-stage decisions consist in deciding the DPs to open and to operate as well as the capacities assigned to DPs from warehouses (i.e., the first echelon of the network) during T periods. In complement, the second-stage decisions look forward to the distribution operations in the second echelon of the network (i.e., from DPs to ship-to-points) and the recourse deliveries. This formulation is referred to as the location and capacity-allocation model (LCA).

The decision variables are defined below:

x_{lpt} = the number of full truckloads assigned from warehouse $p \in \mathcal{P}$ to DP $l \in \mathcal{L}$ at period $t \in \mathcal{T}$.

$y_{lt} = 1$ if DP $l \in \mathcal{L}$ is operating at period $t \in \mathcal{T}$.

$z_{lt} = 1$ if DP $l \in \mathcal{L}$ is opened at period $t \in \mathcal{T}$.

$v_{lj\omega t}$ = fraction of demand delivered from DP $l \in \mathcal{L}$ to ship-to-point $j \in \mathcal{J}$ under demand scenario $\omega \in \Omega_t$.

$s_{j\omega t}$ = fraction of demand of ship-to-point $j \in \mathcal{J}$ satisfied through external delivery under scenario $\omega \in \Omega_t$ of period t (i.e., that ship-to-point is not delivered to from DPs).

We denote the set of feasible combinations of first-stage decisions y_{lt} with y, z_{lt} with z and x_{lpt} with x. Then, the LCA is formulated as a mixed-integer two-stage stochastic linear program:

$$\text{(LCA)} \quad \min_{x,y,z,v,s} \mathbb{E}_\Omega h(x,y,z,\omega) = \min \sum_{t\in\mathcal{T}}\sum_{l\in\mathcal{L}}(f^u_{lt}\, y_{lt} + f^s_{lt}\, z_{lt}) + \sum_{t\in\mathcal{T}}\sum_{l\in\mathcal{L}}\sum_{p\in\mathcal{P}} c_{lpt}\, C_{lp} x_{lpt} + \sum_{t\in\mathcal{T}} \mathbb{E}_{\Omega_t}[Q_t(x,\omega)] \tag{11}$$

$$\text{S. t.} \quad \sum_{l\in\mathcal{L}} C_{lp} x_{lpt} \leqslant C_p \qquad \forall p \in \mathcal{P}, t \in \mathcal{T} \tag{12}$$

$$\sum_{p\in\mathcal{P}} C_{lp} x_{lpt} \leqslant C_l\, y_{lt} \qquad \forall l \in \mathcal{L}, t \in \mathcal{T} \tag{13}$$

$$y_{lt} - y_{lt-1} \leqslant z_{lt} \qquad \forall l \in \mathcal{L}, t \in \mathcal{T} \tag{14}$$

$$x_{lpt} \in \mathbb{N} \qquad \forall l \in \mathcal{L}, p \in \mathcal{P}, t \in \mathcal{T} \tag{15}$$

$$y_{lt}, z_{lt} \in \{0,1\} \qquad \forall l \in \mathcal{L}, t \in \mathcal{T} \tag{16}$$

where $Q_t(x,\omega)$ is the solution of the second-stage problem:

$$Q_t(x,\omega) = \min_{v,s} \sum_{j\in\mathcal{J}} d_{j\omega t}[\sum_{l\in\mathcal{L}} c_{ljt}\, v_{lj\omega t} + c_{j\omega t}\, s_{j\omega t}] \tag{17}$$

$$\text{S. t.} \quad \sum_{j\in\mathcal{J}} d_{j\omega t}\, v_{lj\omega t} \leqslant \sum_{p\in\mathcal{P}} C_{lp} x_{lpt} \qquad \forall l \in \mathcal{L} \tag{18}$$

$$\sum_{l\in\mathcal{L}} v_{jl\omega t} + s_{j\omega t} = 1 \qquad \forall j \in \mathcal{J} \tag{19}$$

$$v_{lj\omega t} \geqslant 0 \qquad \forall l \in \mathcal{L}, j \in \mathcal{J} \tag{20}$$

$$s_{j\omega t} \geqslant 0 \qquad \forall j \in \mathcal{J} \tag{21}$$

The objective function (11) is the sum of the first-stage costs and the expected second-stage costs. The first-stage costs represent the opening DP cost, the operating DP cost, as well as the capacity cost induced by the number of truckloads associated with DPs from warehouses. The objective function of the second stage (17) consists in minimizing the cost of the total flow delivered from DPs to ship-to-points and the cost of the recourse when the ship-to-point is satisfied partially or totally through an extra delivery. Constraints (12) ensure that the quantity delivered from a warehouse do not exceed its capacity. Constraints (13) guarantee the capacity restriction at an operating DP. Constraints (14) define the location setup. To use a DP, opening decisions must be activated in the same period, unless set as active in a preceding period. Constraints (15)-(16) describe the feasible set for the first-stage variables. Constraints (18) aim to cover the ship-to-point demand from the opened DPs. Constraints (19) ensure that a ship-to-point is either satisfied totally or partially through the designed network or from the extra delivery option. Constraints (20)-(21) are the non-negativity constraints for the second-stage variables.

In the LCA model presented above, the first-stage decisions are projected out in the recourse problem through the capacity assignment variables x_{lpt}, as expressed in constraints (18). However, the inclusion of assignment-transportation x_{lpt} as integer first-stage decision variables may complicate its resolution, particularly for large size instances.

4.2. Flow-based location-allocation model (LAF)

As mentioned, the first echelon (warehouses-DPs) distribution operations are represented by a throughput capacity based on the transportation capabilities in the LCA model. Such modeling option necessitates the inclusion of capacity assignment-transportation as the integer first-stage decision variables x_{lpt}, and may complicate its resolution. A common alternative modeling approach is to consider continuous flows as capacity-allocation variables, which are part of the second-stage and thus scenario-dependent variables. In such case, the first echelon distribution operations are represented by a set of origin-destination links, $x_{lpt\omega}$, and refer to the proportion of truckloads assigned from warehouse p to DP l under scenario ω at period t. With such modeling approach, a two-stage stochastic program is obtained where location decisions (opening and operating DPs) are first-stage decisions, and the flow-based transportation decisions in both echelons are second-stage decisions, denoted as the flow-based location-allocation model (LAF). Given the LCA program, constraints (12), (13), and (15) should be adjusted to be part of the recourse problem, and thus replaced by (24), (25), and (28), respectively. Constraint (18) is also substituted by (26). The LAF can then be written as:

$$\text{(LAF)} \min_{y,z,x,v,s} \mathbb{E}_\Omega h(y,z,\omega) = \min \sum_{t\in\mathcal{T}}\sum_{l\in\mathcal{L}}(f^u_{lt}\, y_{lt} + f^s_{lt}\, z_{lt}) + \sum_{t\in\mathcal{T}} \mathbb{E}_{\Omega_t}[Q_t(y,\omega)] \tag{22}$$

$$\text{S. t.} \quad (14) \text{ and } (16)$$

where $Q_t(y,\omega)$ is the solution of the second-stage problem of the LAF formulation:

$$Q_t(y,\omega) = \min_{x,v,s} \sum_{l\in\mathcal{L}}\sum_{p\in\mathcal{P}} c_{lpt}\, C_{lp} x_{lpt\omega} + \sum_{j\in\mathcal{J}} d_{j\omega t}[\sum_{l\in\mathcal{L}} c_{ljt}\, v_{lj\omega t} + c_{j\omega t}\, s_{j\omega t}] \tag{23}$$

$$\text{S. t.} \quad \sum_{l\in\mathcal{L}} C_{lp} x_{lpt\omega} \leqslant C_p \qquad \forall p \in \mathcal{P} \tag{24}$$

$$\sum_{p\in\mathcal{P}} C_{lp} x_{lpt\omega} \leqslant C_l\, y_{lt} \qquad \forall l \in \mathcal{L} \tag{25}$$

$$\sum_{j\in\mathcal{J}} d_{j\omega t}\, v_{lj\omega t} - \sum_{p\in\mathcal{P}} C_{lp} x_{lpt\omega} \leqslant 0 \qquad \forall l \in \mathcal{L} \tag{26}$$

$$\sum_{l\in\mathcal{L}} v_{jl\omega t} + s_{j\omega t} = 1 \qquad \forall j \in \mathcal{J} \tag{27}$$

$$x_{lpt\omega} \geqslant 0 \qquad \forall l \in \mathcal{L}, p \in \mathcal{P} \tag{28}$$

$$v_{lj\omega t} \geqslant 0 \qquad \forall l \in \mathcal{L}, j \in \mathcal{J} \tag{29}$$

$$s_{j\omega t} \geqslant 0 \qquad \forall j \in \mathcal{J} \tag{30}$$

In the LAF model, the recourse problem is linked to the problem by constraints (25), where first-stage decisions are projected out through the operating DP variables (y_{lt}). Given the LCA and LAF models, the next section proposes a solution methodology to solve these two-stage multi-period stochastic versions of the 2E-DDP. Hereafter, we denote for each model $o \in \{\text{LCA, LAF}\}$, the design vector $X(o)$ with $X(\text{LCA}) = \{x, y, z\}$ and $X(\text{LAF}) = \{y, z\}$, respectively.

5. Solution methodology

For real-scale instances of the aforementioned models, one would have to manage the inherent combinatorial complexity and the extremely large set of multi-period demand scenarios of the 2E-DDP under uncertainty. Therefore, our solution approach combines a scenario sampling method and a decomposition schema for stochastic models to find the best solution quality-solvability trade-offs. The sample average approximation (SAA) technique is used to handle the large set of scenarios and sample the most adequate sample size [62]. This approach has been applied to stochastic network design problems in [57, 59, 43]. The detailed adaptation of the technique to our stochastic models is provided in Appendix A.1. Thus, the SAA technique gives a SAA program for each proposed model. Next, we propose a reformulation of both models based on the Benders decomposition scheme [10, 9], adapted to the two-stage and multi-period setting of the stochastic programs produced. Furthermore, the value of the stochastic solution (VSS), the loss using the skeleton solution (LUSS), and the loss of upgrading the deterministic solution (LUDS), proposed in [47], are assessed as indicators of the quality of the stochastic solutions produced. The reformulation of these models and the mathematical functions to measure these indicators are detailed in Appendix A.4. Finally, a scenario-based evaluation procedure is introduced to post-evaluate the alternative design solution produced by the LCA and the LAF models on various problem-instances, and thus discuss their design structure and the quality of the stochastic solutions obtained.

5.1. The Benders decomposition

Given the combinatorial complexity of the stochastic 2E-DDP, cutting plane algorithms such as Benders decomposition could be suitable to enhance its solvability. The Benders decomposition is a well-known partitioning method applicable to mixed-integer programs [10, 9]. In the Benders decomposition, the original problem is separated into a master problem and a number of sub-problems, which are typically easier to solve than the original problem. By using linear programming duality, all sub-problem variables are projected out, and the master problem contains the remaining variables and an artificial variable representing the lower bound on the

cost of each sub-problem. The resulting model is solved by a cutting plane algorithm. In each iteration, the values of the master problem variables are first determined, and the sub-problems are solved with these variables fixed. An optimal solution of the master problem provides a lower bound, and this solution is transmitted to the sub-problems to construct new ones. If the sub-problems are feasible and bounded, an optimality cut is added to the master problem, otherwise a feasibility cut is added. The solution of the feasible sub-problems provides the valid upper bound. By adding the new Benders cuts, the master problem is resolved, and the Benders decomposition algorithm is repeated continuously until the difference between the lower bound and the upper bound is small enough or zero.

In this paper, we introduce a Benders decomposition algorithm to solve the two SAA programs related to the LCA and LAF models based on a set of sampled scenarios Ω^N. In this subsection, we present the Benders reformulation developed for the (LCA(Ω^N)) program and keeping the reformulation for the (LAF(Ω^N)) in Appendix A.2. In the (LCA(Ω^N)) program, integer variables are first-stage decisions, while continuous variables belong to the second-stage. If the first-stage decisions are fixed, the resulting sub-problem can be decomposed into $|T| \times |\Omega^N|$ sub-problems, one for each period $t \in \mathcal{T}$ and each scenario $\omega \in \Omega^N$. This is inspired by the original idea of applying Benders decomposition to stochastic integer programs, also known as the L-shaped method [64, 11]. Given $X(\text{LCA}(\Omega^N)) = \{x, y, z\}$, the fixed vector related to the (LCA(Ω^N)), the expected total cost of the second-stage decisions, denoted with $\phi(x, y, z)$ can be calculated as $\phi(x, y, z) = \frac{1}{N} \sum_{t\in\mathcal{T}} \sum_{\omega\in\Omega_t^N} \phi_{t\omega}(x, y, z)$, where $\phi_{t\omega}(x, y, z)$ is the total second-stage cost for each period t and each scenario ω. This cost is obtained through solving the following primal sub-problem (PS$_{\omega t}$):

$$(\text{PS}_{\omega t}) \quad \phi_{t\omega}(x, y, z) = Q_t(x, \omega) = \min \sum_{j\in\mathcal{J}} d_{j\omega t}[\sum_{l\in\mathcal{L}} c_{ljt}\, v_{lj\omega t} + c_{j\omega t}\, s_{j\omega t}] \tag{31}$$

$$\text{S. t.} \qquad (18) - (21)$$

The (PS$_{\omega t}$) is always feasible because the demand can be satisfied from an extra delivery option, i.e., $s_{j\omega t}$, which is uncapacitated. We denote with α_l and β_j the dual variables associated with constraints (18) and (19), respectively. Accordingly, the dual of (PS$_{\omega t}$) for each t and ω, called the dual sub-problem (DS$_{\omega t}$), can be formulated as:

$$(\text{DS}_{\omega t}) \quad \phi_{t\omega}(x, y, z) = \max \sum_{l\in\mathcal{L}} \sum_{p\in\mathcal{P}} C_{lp}\, x_{lpt}\, \alpha_l + \sum_{j\in\mathcal{J}} \beta_j \tag{32}$$

$$\text{S. t.} \qquad d_{j\omega t}\, \alpha_l + \beta_j \leqslant d_{j\omega t}\, c_{ljt} \qquad \forall l \in \mathcal{L}, j \in \mathcal{J} \tag{33}$$

$$\beta_j \leqslant d_{j\omega t}\, c_{j\omega t} \qquad \forall j \in \mathcal{J} \tag{34}$$

$$\alpha_l \leqslant 0 \qquad \forall l \in \mathcal{L} \tag{35}$$

$$\beta_j \in \mathbb{R} \qquad \forall j \in \mathcal{J} \tag{36}$$

We define as $\Delta_{t\omega}$ the polyhedron under the constraints (33) and (34) of (DS$_{\omega t}$). Let $P_{\Delta_{t\omega}}$ be the set of extreme points of $\Delta = \cup_{t\omega}\Delta_{t\omega}$. We introduce an additional variable $u_{t\omega}$ representing the total expected second-stage decision cost per t and ω. Thus, the Benders master problem is written as:

$$\text{(BMP)} \min \sum_{t\in\mathcal{T}} \sum_{l\in\mathcal{L}} (f_{lt}^u\, y_{lt} + f_{lt}^s\, z_{lt}) + \sum_{t\in\mathcal{T}} \sum_{p\in\mathcal{P}} \sum_{l\in\mathcal{L}} c_{lpt} C_{lp} x_{lpt} + \frac{1}{N} \sum_{t\in\mathcal{T}} \sum_{\omega\in\Omega_t^N} u_{t\omega} \tag{37}$$

$$\text{S. t.} \qquad (12) - (16)$$

$$u_{t\omega} - \sum_{l\in\mathcal{L}} \sum_{p\in\mathcal{P}} C_{lp}\, x_{lpt}\, \alpha_l \geqslant \sum_{j\in\mathcal{J}} \beta_j \qquad \forall t \in \mathcal{T}, \omega \in \Omega_t^N,\ (\alpha_l, \beta_j) \in P_{\Delta_{t\omega}} \tag{38}$$

$$u_{tw} \geqslant 0 \qquad \forall t \in \mathcal{T}, \omega \in \Omega_t^N \tag{39}$$

Constraints (38) represent the Benders optimality cuts.

5.2. Evaluation procedure

When using a sampling approach, the assessment of the design solutions produced by the two models presented in Section 4 is restricted to the set of scenarios considered. To better appreciate the performance of the produced design solutions, we develop a complementary evaluation procedure. This relies on the fact that the higher the evaluation sample size, the more precise the assessment of the design solution. It also builds on the ability of this post-optimization phase to introduce additional performance measures to appreciate the robustness of the solution, which were not part of the optimized model. In practice, a design solution evaluation procedure would be as close as possible to the company's real operational problem. Hereafter, we consider the second-stage formulation of the LCA and LAF models as an evaluation model that practically refers to operational-level decisions. In addition, we base the evaluation on a much larger sample of Monte Carlo scenarios, $N^e \gg N$ ($N^e = |\Omega_t^{N^e}|$), than those used to generate the candidate designs. Thus, for a given design vector $\widehat{X}_t(o)$ at period t obtained from the SAA program $o \in \{\text{LCA}(\Omega^N), \text{LAF}(\Omega^N)\}$, we compute the cost value for each scenario $\omega \in \Omega_t^{N^e}$, $Q_t(\widehat{X}_t(o), \omega)$, using the respective sub-model. More specifically, in the (LCA(Ω^N)) program, the design vector is $\widehat{X}_t(\text{LCA}(\Omega^N))=\{\hat{x}_t, \hat{y}_t, \hat{z}_t\}$, and the $Q_t(\widehat{X}_t(\text{LCA}(\Omega^N)), \omega)$ is evaluated by (17)-(21). On the other hand, for (LAF(Ω^N)), the design vector is $\widehat{X}_t(\text{LAF}(\Omega^N))=\{\hat{y}_t, \hat{z}_t\}$, and the $Q_t(\widehat{X}_t(\text{LAF}(\Omega^N)), \omega)$ is evaluated by (23)-(30). We notice that the evaluation model is separable per scenario since the design decisions are fixed. This then allows considering a much larger scenarios sample.

First, a measure of the expected value $\mathcal{V}_t^e(o)$ for each design period t is computed using the evaluation sample Ω^{N^e}. Second, a downside risk measure is computed to assess the variability of each design at period t. More specifically, the variability measure is the upper semi-deviation from the mean, $MSD_t(o)$, for each model $o \in \{\text{LCA}(\Omega^N), \text{LAF}(\Omega^N)\}$, and is formulated as:

$$MSD_t(o) = \frac{1}{N^e} \sum_{\omega=1,\ldots,N^e} \max\left(0; Q_t(\widehat{X}_t(o), \omega) - \mathbb{E}_{\Omega^{N^e}}[Q_t(\widehat{X}_t(o), \omega)]\right)$$

This measure was introduced by Shapiro et al. in [62], and helps assess the penalization of an excess of a realization ω over its mean. The evaluation procedure is detailed in the algorithms 1 and 2 for LCA(Ω^N)and LAF(Ω^N), respectively.

Algorithm 1 Evaluation procedure LCA(Ω^N) model

for all $t = 1, \ldots, T$ **do**
  for all $\omega = 1, \ldots, N^e$ **do**
    Evaluate $Q_t(\widehat{X}_t(LCA(\Omega^N)), \omega)$ using the program (17)-(21)
  end for
  Evaluate $\mathcal{V}_t^e(LCA(\Omega^N)) = \sum_{l \in \mathcal{L}} (f_{lt}^u \, \hat{y}_{lt} + f_{lt}^s \, \hat{z}_{lt}) + \sum_{l \in \mathcal{L}} \sum_{p \in \mathcal{P}} c_{lpt} \, C_{lp} \hat{x}_{lpt} + \mathbb{E}_{\Omega_t^{N^e}}[Q_t(\widehat{X}_t(LCA(\Omega^N)), \omega)]$
  Evaluate $MSD_t(LCA(\Omega^N))$
end for

Algorithm 2 Evaluation procedure for LAF(Ω^N) model

for all $t = 1, \ldots, T$ **do**
  for all $\omega = 1, \ldots, N^e$ **do**
    Evaluate $Q_t(\widehat{X}_t(LAF(\Omega^N), \omega)$ using the program (23)-(30)
  end for
  Evaluate $\mathcal{V}_t^e(LAF(\Omega^N)) = \sum_{l \in \mathcal{L}} (f_{lt}^u \, \hat{y}_{lt} + f_{lt}^s \, \hat{z}_{lt}) + \mathbb{E}_{\Omega_t^{N^e}}[Q_t(\widehat{X}_t(LAF(\Omega^N)), \omega)]$
  Evaluate $MSD_t(LAF(\Omega^N))$
end for

6. Computational results

In this section, we describe the experimental study carried out and the related results. First, we present the data instances used in the experiments. Second, we provide the calibration of the design models using the SAA

method. Then, we discuss the results in terms of the solvability of the stochastic models and the value of the stochastic solutions. Third, we summarize the obtained results and evaluate the different designs produced by the two models in terms of design structure and design value. All experiments were run using a cluster Haswell Intel Xeon E5-2680 v3 2.50 GHz of two processors with 12 Cores each and 128 Go of memory. We used CPLEX 12.7 to solve the linear programs.

6.1. Test data

In our experiments, we generated several 2E-DDP instances based on the following factors: the problem size, the network characteristics, and the demand processes. The tested size problems are shown in Table 2. The network incorporates several possible configurations depending on the number of different DP locations (# DPs) and the number of different capacity configurations per DP location (# capacity configurations). Thus, multiplying these two parameters gives the number of potential DPs, $|\mathcal{L}|$. In the case of several capacity configurations, the second configuration has a higher capacity. Ship-to-points are realistically scattered in the geographic area covered ($160000\,km^2$). The number of warehouses ($|\mathcal{P}|$) is also given. A 5-year planning horizon is considered in this context, which is partitioned into 5 design periods in the tests (i.e., $|\mathcal{T}| = T = 5$).

Table 2: Test problems size

Problem instance (P)	$\|\mathcal{J}\|$	$\|\mathcal{P}\|$	# DPs	# capacity configurations	$\|\mathcal{L}\|$
P1	50	2	4	1	4
P2	50	3	8	1	8
P3	50	4	8	2	16
P4	75	3	8	1	8
P5	75	4	8	2	16
P6	100	3	8	1	8
P7	100	4	8	2	16

We consider simple and compound demand processes. The simple process refers to a normally distributed demand level per ship-to-point j and per period t. The compound process refers to a Bernoulli-normal distribution, where the Bernoulli process shapes the demand occurrence for a given ship-to-point j at period t with a probability p_{jt}, $j \in \mathcal{J}$, $t \in \mathcal{T}$. In both processes, the normal distribution refers to the demand quantity with a mean value μ_{jt} and a standard deviation σ_{jt}, $j \in \mathcal{J}$, $t \in \mathcal{T}$. In addition, we consider a network including large-size (L) and medium/small-size (S) ship-to-points reflected by the historical mean value μ^L_{j0} and μ^S_{j0} for a given ship-to-point j, respectively. We set large-size ship-to-points that represent 20% of the network with an associated demand occurrence rate of $p^L_{jt} = 0.95$ (in contrast to a rate of $p^S_{jt} = 0.8$ for small-size ship-to-points). Moreover, we assume that each ship-to-point mean demand μ_{jt} depends on a time varying trend, based on a factor δ_j and on the historical mean μ_{j0}. The coefficient of variation ($\frac{\sigma_{jt}}{\mu_{jt}}$) is a fixed parameter for each ship-to-point over periods. Two alternative time-varying trends are tested here with respect to the two demand processes to obtain the three problem instances shown in Table 3. The normal distribution with a regular trend (NRT) refers to a ship-to-point mean value that is related to the historical mean at $t = 0$, and following a regular inflating factor δ_j over the periods of the planning horizon. The same regular trend is applied with the compound Bernoulli-normal distribution and is denoted with CRT. Finally, the normal distribution with a dynamic trend (NDT) refers to the case where each ship-to-point mean demand varies dynamically over periods according to a perturbation factor δ_{jt} linked to the preceding period. The values and ranges for all the parameters with regard to the demand process are given in Table 3.

Warehouse and DP capacities are uniformly generated with respect to the demand level of the problem instance in the unit intervals $[25k, 32k]$ and $[7k, 11k]$, respectively. The truckload capacities between warehouses and DPs are estimated in the interval $[1700, 2500]$. High and low levels of fixed costs are defined and denoted with LL and HL, respectively. The fixed costs for each DP are generated per period t, respectively in the ranges $[100k, 150k]$ and $[3500, 6500]$, proportionally to its maximum capacity. An inflation factor is also considered to reflect the increase of the cost of capital on a periodic basis with $r = 0.005$. All the locations of the network

Table 3: Demand processes

Normal distribution	NRT	$\mu_{jt} = \mu_{j0}(1 + \delta_j \times t)$	$\delta_j \in [0, 0.1]$
	NDT	$\mu_{jt} = \mu_{jt-1}(1 + \delta_{jt})$	$\delta_{jt} \in \{0.15, -0.2, 0\}$
Compound Bernoulli-Normal distribution	CRT	$\mu_{jt} = \mu_{j0}(1 + \delta_j \times t)$	$\delta_j \in [0, 0.1]$
$\mu^L_{j0} \in [300; 400]$, $\mu^S_{j0} \in [150; 220]$, $\frac{\sigma_{jt}}{\mu_{jt}} = 0.25$, $p^L_{jt} = 0.95$ and $p^S_{jt} = 0.8$			

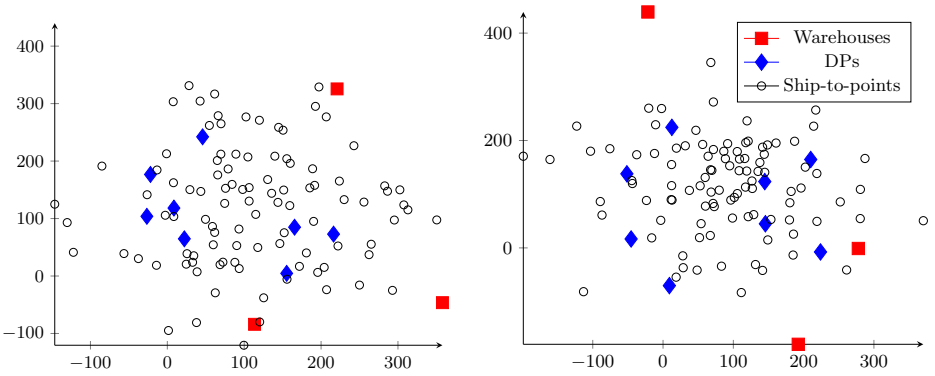

(a) Dispersed ship-to-points instance (Dis) (b) Concentric ship-to-points instance (Con)

Figure 4: Ship-to-points scattering in the space for P6

(warehouses, DPs, ship-to-points) are normally scattered in a given space as shown in the instances of Figure 4. As illustrated, we separate in the instances two possible configurations according to the disposition of the ship-to-points: dispersed (Dis) or concentric (Con). The transportation costs between the network nodes correspond to the Euclidean distances, multiplied by a unit load cost per distance unit and the inflation factor r. The unit load cost per distance unit is different in each echelon to reflect the different loading factors. The external delivery cost c_{jt} is calibrated to be higher than internal distribution costs with $c_{jt} \in [2200; 3000]$). To apply the SAA technique, we used in our experiments $M = 6$ samples, a reference sample $N' = 2000$, and running $N \in \{100, 200, 500\}$ generated scenarios. We refer to $s \in \{s1, s2, \ldots, s6\}$ as the sample used, and denote with $\bar{s}$ the average value over the 6 samples. We considered an evaluation sample size $N^e = 2000$.

Combining all the elements above yielded 84 problem instances. Each instance type is a combination of $(a, b, c, d), a \in \{Dis, Con\}, b \in \{P1, P2, P3, P4, P5, P6, P7\}$, $c \in \{LL, HL\}$, $d \in \{NRT, NDT, CRT\}$. Each instance problem is denoted by the ship-to-points configuration a, the problem size b, the cost level c, the demand process d, the sample size N, and its references s. It has the format a-b-c-dNs (for example, Dis-P1-LL-NRT-500s1).

6.2. Results

6.2.1. Models' solvability analysis

The first solution quality-seeking step for stochastic models is the calibration of the number N of scenarios to include in the optimization phase. Such calibration is carried out using the SAA algorithm 3 in Appendix A.1, and the quality of the obtained solutions is evaluated using the statistical optimality gap. Table 4 summarizes the average optimality gap values for the sample size $N = 500$ for the medium and large problem instances (P4 to P7). The optimality gap is expressed as a percentage of the objective function value of the best design found for a given instance. The results for $N \in \{100, 200\}$ and for P1 to P3 are given in Table B.11 of Appendix B.

We can see in this table that (LCA(Ω^N)) provides satisfactory results, generally less than 1% for most instances starting from $N = 500$, for all the demand processes investigated. Our experiments show that the optimality gap value improves as the sample size N grows and converges to 0%, as illustrated in Table B.11 of Appendix B. Moreover, we note that the design solutions produced with alternative samples ($M = 6$) of 500 scenarios provide the same location decisions. In the same way, regarding the (LAF(Ω^N)) model, the results

Table 4: Average statistical optimality gap values for P4-P7

	$gap^{500,2000}$ (%)	
	LCA(Ω^N)	**LAF(Ω^N)**
P4-NRT-LL-500$\bar{s}$	0.05	0.02
P4-NDT-LL-500$\bar{s}$	0.01	0.01
P4-CRT-LL-500$\bar{s}$	0.28	-0.04
P5-NRT-LL-500$\bar{s}$	0.08	0
P5-NDT-LL-500$\bar{s}$	0.16	0.01
P5-CRT-LL-500$\bar{s}$	0.31	-0.04
P6-NRT-LL-500$\bar{s}$	0.14	0
P6-NDT-LL-500$\bar{s}$	0.12	-0.01
P6-CRT-LL-500$\bar{s}$	0.29	-0.01
P7-NRT-LL-500$\bar{s}$	0.18	0
P7-NDT-LL-500$\bar{s}$	0.01	0.01
P7-CRT-LL-500$\bar{s}$	0.16	-0.01

Table 5: Evaluation of the stochastic solution

	P2-		P4-		P6-	
Indicators	LCA(Ω^N)	LAF(Ω^N)	LCA(Ω^N)	LAF(Ω^N)	LCA(Ω^N)	LAF(Ω^N)
LL-NRT-500$\bar{s}$						
$\widehat{VSS}$(%)	22.82	8.13	45.47	0.6	95.98	0
$\widehat{LUSS}$(%)	13.67	8.13	0	0.6	26.3	0
$\widehat{LUDS}$(%)	4.13	0.51	0	0.16	1.2	0
LL-NDT-500$\bar{s}$						
$\widehat{VSS}$(%)	3.85	0	93.63	0	101.42	0
$\widehat{LUSS}$(%)	2.33	0	28.6	0	0.87	0
$\widehat{LUDS}$(%)	0.95	0	3.38	0	1.0	0
LL-CRT-500$\bar{s}$						
$\widehat{VSS}$(%)	89.49	0	57.08	0	222.01	0.04
$\widehat{LUSS}$(%)	11.26	0	11.7	0	0.09	0.04
$\widehat{LUDS}$(%)	0.59	0	1.62	0	0.4	0.04

show a very low gap, almost less than 0.1%, which underlines the sufficiency of this sample size. Accordingly, the sample size of $N = 500$ scenarios is considered satisfactory in terms of solvability and solution quality, and retained for the rest of the experiments with both models (LCA(Ω_N)) and (LAF(Ω_N)).

With this in mind, we next propose exploring the deterministic counterparts of both models and evaluate the difference between the deterministic and the stochastic solutions using the indicators proposed in [47]. These indicators are detailed in Appendix A.4. Table 5 provides an evaluation of the estimated value of stochastic solution ($\widehat{VSS}$), the estimated loss using the skeleton solution ($\widehat{LUSS}$), and the estimated value of loss of upgrading the deterministic solution ($\widehat{LUDS}$) as a percentage of the expected value of the recourse problem ($\widehat{RP}$) for problem sizes P2, P4, and P6 with both models.

Table 5 highlights a large value for the $\widehat{VSS}$ compared to $\widehat{RP}$ in the (LCA(Ω^N)) program, and a lower value in the (LAF(Ω^N)) program: it can reach 96% in the (LCA(Ω^N)) with problem size (P6), and 8% in (LAF(Ω^N)) with (P4), under the NRT demand process. The large $\widehat{VSS}$ values obtained in some cases with (LCA(Ω^N)) are partly due to the high variability of the objective function value for these instances. This variability is due to the information assumed when the capacity-allocation decisions of all the periods are anticipated at the first-stage. Conversely, this effect is attenuated in the case of (LAF(Ω^N)) because the capacity-allocation decisions are scenario-dependent and thus part of the recourse problem.

Regarding the skeleton solution from the deterministic model, we obtain $\widehat{ESSV}$ equal to or higher than

Table 6: The average computational time (CPU)

P	**LCA(Ω^N)**						**LAF(Ω^N)**				
	Variables			Constraints	CPU		Variables		Constraints	CPU	
	Binary	Integer	Continuous		DEF	BD	Binary	Continuous		DEF	BD
P1	40	80	625000	135050	23m7s	2m54s	40	645000	150020	9m49s	2m29s
P2	80	120	1125000	145095	9h10m	47m49s	80	1185000	172540	2h11m	10m23s
P3	160	320	2125000	145180	35h20m	13h3m	160	2285000	285080	21h30m	1h17s
P4	80	120	1687500	187595	10h38m	1h5m43s	80	1747500	235040	4h	14m41s
P5	160	320	3187500	187180	-	15h15m	160	3347500	347580	-	2h53m
P6	80	120	2250000	270095	39h42m	2h15m	80	2310000	297540	8h26m	20m45s
P7	160	320	4250000	270180	-	40h40m	160	4410000	410080	-	5h

-: Not solved within time limit 48 hours

$\widehat{RP}$ in the (LCA(Ω^N)) model. This leads to a $\widehat{LUSS}$ greater than zero, but remains less than the $\widehat{VSS}$ (i.e., $0 < \widehat{LUSS} \leqslant \widehat{VSS}$). The positive $\widehat{LUSS}$ obtained in our evaluation of the (LCA(Ω^N)) model means that the deterministic solution tends to open non-optimal DPs, and sub-optimally allocate DP capacity from warehouses. The same statement is observed with (LAF(Ω^N)) where the variability reaches 8% under the NRT demand process. In addition, for many problem instances with the (LAF(Ω^N)) program, the perfect skeleton solution is captured. The last measure evaluates the upgradability of the deterministic solution to the stochastic solution. The table indicates that (LCA(Ω^N)) presents a small and non-zero $\widehat{LUDS}$ value (about 4% and 1% for P2 and P6, respectively, in (LCA(Ω^N)) and less than 0.5% for P2 in (LAF(Ω^N)). This confirms the non-upgradability of the deterministic solution for problem sizes P2 and P6. The results using the NDT and the CRT demand processes also validate the high value of the stochastic solution compared to the deterministic counterpart for (LCA(Ω^N)). In this case, the $\widehat{VSS}$ value increases as the demand variability grows, and reaches 200% of the $\widehat{RP}$ for the CRT demand process. On the other hand, the (LAF(Ω^N)) model shows a low variability of the stochastic solutions with the NDT and CRT demand processes. These primary results show the value of investigating the stochastic formulations of the 2E-DDP. One may also conclude that (LCA(Ω^N)) is much more sensitive to demand uncertainty due to the anticipation of the capacity-allocation decisions at the first stage.

Finally, solvability is a crucial issue that needs to be taken into consideration given the complexity of stochastic programming models. Table 6 provides the average computational time (CPU) for the two proposed models. It compares the running time of the deterministic equivalent formulation (DEF) when solving with a commercial solver (Cplex) and when applying the Benders decomposition (BD). The results show the efficiency of the BD approach in considerably reducing the running time. The BD running time is 4 to 18 times less than using Cplex for DEF for (LCA($C\Omega^N$)) where the higher difference (18 times faster) is observed for P6. In the case of (LAF(Ω^N)), the efficiency of BD is also significant, namely, 25 times faster for P6. Moreover, the table indicates that the CPU(s) grows as the problem size increases, clearly a further complexity with P3, P5, and P7 where two capacity configurations are considered. We also observe that (DEF) cannot be solved to optimality for problem instance (P5) and (P7) within the time limit of 48 hours. Nevertheless, the (P7) problem instance is solved to optimality with the BD approach within 40 hours and 5 hours for the (LCA(Ω^N)) and the (LAF(Ω^N)) model, respectively. Further, Table 6 confirms the huge discrepancy between the solved models in terms of complexity and consequently running times. The (LAF(Ω^N)) program seems easier to tackle, where the CPU(s) is 3 to 12 times less than in (LCA(Ω^N)). The high computational time observed in (LCA(Ω^N)) is mainly due to the complexity of the integer capacity variables, and thus the combinatorial nature in the problem, which makes it intractable for larger instances. These results also confirm the importance of the development of the Benders decomposition approach to solve a large scale 2E-DDP.

6.2.2. Design solutions analysis

In this subsection, we provide an analysis of the design solutions produced by the two models proposed to deal with the stochastic 2E-DDP. Three facets are relevant: 1) the global performance of the design solutions in terms of the expected value and the expected mean semi-deviation (MSD) value, 2) the sensitivity of DP

location decisions to uncertainty under various problem attributes, and 3) the behavior of the capacity-allocation decision in a multi-period and uncertain setting. These analyses are based on the numerical results of the 84 problem instances described above. We recall that the evaluation is based on the procedures given in 1 and 2 for the LCA and LAF models, respectively, with a large evaluation sample of $N^e = 2000$ scenarios.

Design solutions performance

To start, Table 7 describes relative deviations to the best value recorded on the expected value, and the MSD for the (LCA(Ω^N)) model using large-size problems (P6 and P7) contrasted with the NRT, NDT, and CRT demand processes. When looking at the solutions' performance in terms of expected value, we observe that the designs produced by the alternative samples present a small deviation, often less than 0.5%, which clearly indicates the stability of the design structure over the samples. Verter and Dincer in [66] show that location decisions tend to be highly driven by the network topology, as is the case in our results. The highest deviations observed are 0.48% for P6-CRT and 1.87% for P7-NDT, deriving from the slightest sensitivity of the capacity-allocation decisions to the optimization sample. When inspecting the MSD measure, we observe a higher deviation between the design solutions, which is due to the relatively small mean semi-deviation values (about 8k). Also, we underline that for a given problem instance, the design solution presenting the lowest MSD is generally different from that providing the lowest expected value. This offers distribution network designers a better insight with regard to Pareto optimality. As illustrated in Table 7, these observations are still valid under all the demand processes and network typologies. For problem sizes P2 to P5, the results led to similar conclusions and are detailed in Tables B.12 and B.13 in Appendix B. In the case of the (LAF(Ω^N)) model, the mean value and MSD deviation results indicate a pronounced similarity in the design structure, since all the samples lead to the same design value. This is clearly due to modeling the capacity decisions as scenario-dependent in the second stage in (LAF(Ω^N), which bases the design evaluation only on the location decisions. Therefore, one can conclude that the DP location is well stabilized, but the capacity-allocation decisions are sensitive to the demand scenarios. These results are congruent with the insights derived from the statistical gaps, and confirm the good quality solutions produced by both design models.

Table 7: Mean value and MSD deviations for (LCA(Ω^N)) under (P6,P7)-LL-500 attributes

		P6-LL-500						**P7-LL-500**					
		NDT		**NRT**		**CRT**		**NDT**		**NRT**		**CRT**	
		% $\mathcal{V}^e$	% MSD	% $\mathcal{V}^e$	% MSD	% $\mathcal{V}^e$	% MSD	% $\mathcal{V}^e$	% MSD	% $\mathcal{V}^e$	% MSD	% $\mathcal{V}^e$	% MSD
Dis-	s1	0.14	**0**	**0**	1.06	0.48	15.37	0.13	3.93	0.02	**0**	0.31	38.2
	s2	0.19	28.50	0.11	12.97	0.05	**0**	0.11	11.5	**0**	6.88	0.02	**0**
	s3	**0**	5.15	**0**	1.06	**0**	6.09	0.09	17.52	0.07	13.36	**0**	8.04
	s4	0.11	15.65	0.02	3.21	0.1	11.99	0.15	15.45	0.42	79.87	0.02	2.73
	s5	0.15	33.6	**0**	1.06	0.2	1.3	**0**	**0**	0.06	12.27	0.01	0.48
	s6	0.21	49.19	0.04	**0**	0.05	0.77	0.04	4.01	0.16	24.72	0.51	42.26
Con-	s1	0.06	3.87	0.31	69.10	0.05	6.09	**0**	94.33	0.49	107.16	**0**	6.89
	s2	**0**	6.10	**0**	19.82	0.11	7.99	**0**	94.33	0.45	3.84	0.52	36.24
	s3	0.15	27.67	0.03	9.43	**0**	**0**	1.87	**0**	0.48	**0**	0.16	8.71
	s4	0.20	47.90	**0**	19.82	0.10	13.38	**0**	94.33	0.19	4.73	0.04	1.33
	s5	**0**	6.10	0.21	**0**	0.40	30.02	**0**	94.33	**0**	19.17	0.12	14.27
	s6	0.05	**0**	**0**	19.82	0.11	7.99	0.32	87.98	0.15	6.56	0.22	**0**

Location decisions sensitivity

Next, we look closely at the design decisions produced by both models presented in Tables 8 and 9 for medium- and large-size problems (P4 to P7) with (LCA(Ω^N)) and (LAF(Ω^N)), respectively. We note that the represented design corresponds to the best solution in terms of expected value based on Table 7. For each demand process, these tables provide DP opening decisions and their capacity configuration, where value

Table 8: Best location decisions for (LCA(Ω^N))

	Dispersed ship-to-points (Dis)																											
	NRT-500								NDT-500								CRT-500											
DPs	**l1**	**l2**	**l3**	**l4**	**l5**	**l6**	**l7**	**l8**	**l1**	**l2**	**l3**	**l4**	**l5**	**l6**	**l7**	**l8**	**l1**	**l2**	**l3**	**l4**	**l5**	**l6**	**l7**	**l8**				
P4-LL	1			1	1		1		1					1	1		1			1			1					
P4-HL	1			1		1	1		1					1	1		1					1	1					
P5-LL	1			1	1		1		1					1	1		1					1	2					
P5-HL	1					2	2		1					1	1		1					1	2					
P6-LL		1				1	1			1				1	1			1				1	1					
P6-HL		1				1	1			1				1	1			1				1	1					
P7-LL		1				1	2			1				1	1			1				1	1					
P7-HL		1				1	1				2	2						1				1	1					
Concentric ship-to-points (Con)																												
P4-LL	1		1		1	1			1				1		1		1				1		1					
P4-HL	1				1		1		1				1		1		1				1		1					
P5-LL	1				2		2		1				1		1		1				1		1					
P5-HL	1				2		2						1	1	1		1				1		1					
P6-LL	1						1	1	1						1	1	1						1	1				
P6-HL	1						1	1						1	1	1	1		1					1				
P7-LL	1						2	1							2	2	1						1	1				
P7-HL	1						2	1							2	2	1		1					1				

1 corresponds to an opened DP with a low capacity configuration, 2 refers to a high capacity configuration, and blanks refer to DPs kept closed. The third row corresponds to the list of potential DPs and the first column lists the instance labels in terms of problem size and cost structure. The first part of the tables is dedicated to instances with dispersed ship-to-points, and the second part depicts instances with concentric ship-to-points. First, Tables 8 and 9 show that the opened DP number is quite stable in the instances, but the location of DPs and the capacity level are correlated with the demand process, the ship-to-point dispersion, and the DP fixed cost. In almost all the instances, DP locations 6 and/or 7 are opened, because they benefit from a centralization effect due to their positioning in the grid (see Figure 4) and the importance of inbound and outbound transportation costs. Table 8 also reveals the impact of the opening DP costs on the strategic location decisions where in several cases the design structure varies between high and low DP opening costs. For instance, we observe in Table 8 that with P5-LL-Dis-NRT the network design opens four DPs at capacity level 1, whereas with P5-HL-Dis-NRT, only three DPs are opened, but two at capacity level 2. Additionally, the results point out the impact of ship-to-point dispersion (i.e., Dis vs Con) on the DP location decisions, mainly under LL attributes. For instance, DPs 7 and 8 are opened with P7-HL-Dis-NDT instead of DPs 3 and 4 with P7-HL-Con-NDT. In the same way, Table 9 reports different design solutions for all P7 instances and several P5 instances for the LAF(Ω^N) model, which are the problems considering two capacity levels, and thus offer more distribution capabilities to deal with demand uncertainty.

Moreover, a key finding is the sensitivity of the network design in terms of the opened DPs and their location with respect to demand uncertainty. First, essential to mention is that all the opening decisions depicted in these figures are fixed from the first design period and no further opening are made at periods two to five. This behavior is explained by the fact that the DP opening costs follow an increasing trend function along the planning horizon. It is thus more efficient to anticipate future DP openings, if any, at design period one. This anticipation effect is only possible with the explicit modeling of a multi-period design setting, as is the case in this work, in contrast to a static modeling approach to design decisions. In addition, these results reveal that the number of opened DPs under the three demand processes is in general the same for a given problem size. However, for some instances, the number of DPs under NRT is higher than the two other demand processes. Considering instance P4-LL-Dis, four DPs are opened under NRT, whereas only three DPs are opened with NDT and CRT. This behavior is observed for both the LCA and LAF models' solutions. It can be seen as the flexibility hedging of both models to avoid opening additional DPs when uncertainty increases. We also note a high variability in the location of opened DPs when comparing solutions from the different demand processes. To emphasize this result, one can closely observe the instance P4-LL-Dis, where we obtain 66.7% identical DPs for NDT vs CRT, 50% for NRT vs NDT, and 75% for NRT vs CRT, when the LCA model is solved. Similarly,

Table 9: Best location decisions for (LAF(Ω^N))

	Dispersed ship-to-points (Dis)																							
	NRT-500								**NDT-500**								**CRT-500**							
DPs	**l1**	**l2**	**l3**	**l4**	**l5**	**l6**	**l7**	**l8**	**l1**	**l2**	**l3**	**l4**	**l5**	**l6**	**l7**	**l8**	**l1**	**l2**	**l3**	**l4**	**l5**	**l6**	**l7**	**l8**
P4-LL	1			1	1		1		1					1	1		1					1	1	
P4-HL	1					1	1		1					1	1		1					1	1	
P5-LL	2					1	1		1					1	1		1					1	1	
P5-HL	2					1	1		1					1	1		1					1	1	
P6-LL		1				1	1			1				1	1			1				1	1	
P6-HL		1				1	1			1				1	1			1				1	1	
P7-LL		1				1	1			1				1	1			1				1	1	
P7-HL		1				1	1			1				1	1			1				1	1	
Concentric ship-to-points (Con)																								
P4-LL	1				1		1				1		1	1					1		1	1		
P4-HL	1				1		1				1		1	1					1		1	1		
P5-LL	1				1		1				1		1	1					1		1	1		
P5-HL	1				1		1				1		1	1					1		1	1		
P6-LL	1						1	1	1		1					1					1		1	1
P6-HL					1		1	1						1	1	1						1	1	1
P7-LL	1						1	1							2	2					1		1	1
P7-HL					1		1	1						1	1	1						1	1	1

Table 10: The impact of capacity configuration on the location decisions

	P2-LL vs P3-LL		P4-LL vs P5-LL		P6-LL vs P7-LL	
	%loc	%cap	%loc	%cap	%loc	%cap
NRT	75%	79.17%	75%	62.5%	75%	75%
CRT	70.83%	45.83%	100%	100%	83.33%	58.33%
NDT	70.83%	41.67%	79.17%	64.58%	97.22%	100%

when the LAF model is solved, we obtain 50% of identical DPs for both NRT vs NDT, and NRT vs CRT, and 100% for CRT vs NDT. The worst case is observed for instance P6-HL-Con with only 33.3% identical DPs for NDT vs CRT, and 66.7% for NRT vs NDT, and for NRT vs CRT with the LCA model. These results confirm that the stochastic multi-period demand process is adequately captured by both the two-stage reformulations of the multi-stage problem.

In complement to the above analysis, Table 10 provides similarity statistics on DPs opening and their capacity level for several pairs of instances when LCA is solved. In general, we observe a very high similarity in the DPs' location, over 70% identical positions, but a much lower similarity in the capacity configuration (about 40%). Looking closely at instance P7-LL-Con, we see that CRT and NDT give two identical DPs location out of three, but these identical DPs are not opened at the same capacity configuration level. Therefore, the results confirm the high variability in solutions in terms of location when capacity levels are considered, and the sensitivity of the two-echelon capacitated distribution network to uncertainty.

Capacity-allocation decision behavior

Furthermore, we discuss the behavior of the capacity-allocation decisions in a multi-period and uncertain setting. Figure 5 examine in depth the capacity decisions modeled in the LCA model and contrast it to the evolution of each demand process along the planning horizon. This figure provides the results of the instance P6-LL-Dis for the three demand processes, which for all cases produced a design solution with three opened DPs. Each solid line corresponds to the capacity level allocated to an opened DP (i.e., $\sum_p C_{lp} x_{lpt}$) for each design period t, and each dashed line its related predetermined capacity C_l (each color distinguishes a separate opened DP). Figure 5 clearly illustrates the impact of the multi-period modeling approach where the capacity-allocation decisions for each opened DP are clearly adapted periodically. Even if for the three demand processes of this instance the LCA model produces the same DP location decisions, the capacity-allocation decisions behave

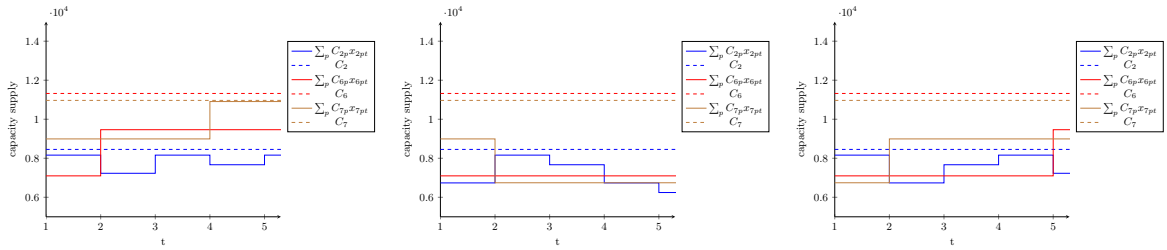

(a) NRT process (b) NDT process (c) CRT process

Figure 5: Capacity-allocation decisions versus the a priori capacity C_l for Dis-P6-LL-500 in (LCA(Ω^N))

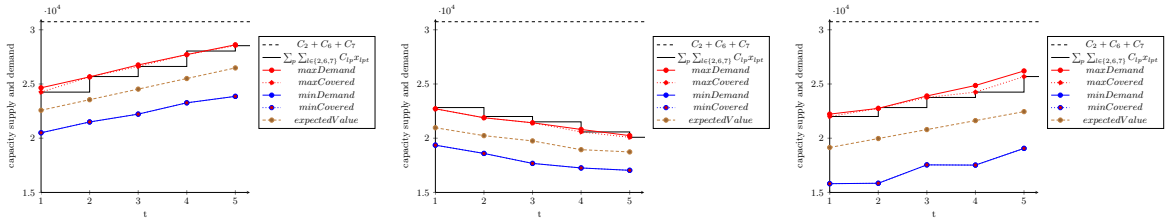

(a) NRT process (b) NDT process (c) CRT process

Figure 6: Capacity decisions versus demand for Dis-P6-LL-500 in (LCA(Ω^N))

differently under each demand process to follow the time-varying demand process. This means that the two-stage LCA mimics the dynamic capacity model with the inclusion of multi-period capacity-allocation decisions.

Figure 6 completes the analysis, with the same instance under the three demand processes: it aggregates the capacity-allocation $\sum_l \sum_p C_{lp}x_{lpt}$ over all the opened DPs at each period t (solid line in black) and the capacity limit $\sum_l C_l$ (dashed line). The figure contrasts the global network capacity with the average demand scenario, the maximum demand scenario, and the minimum demand scenario. It also illustrates the relation between these typical scenarios and the effective demand covered by the opened DPs with a dotted line (i.e., $\sum_{j=1..|\mathcal{J}|} d_{j\omega t} \sum_{l=1..|\mathcal{L}|} v_{lj\omega' t}$, at each t, as formulated in constraint (13). The main insight here is that the capacity-allocation decisions follow the periodic demand under the regular, and most importantly, the dynamic demand setting. This insight is accentuated by the observation that the capacity-allocation decisions follow in all cases the maximum demand scenario. This means that this first-stage decision takes into account the worst case demand (highest demand scenario) and provides the necessary capacity to hedge against it. Clearly, this latter point means that the capacity available at DPs at each period precedes the minimum and the expected demand scenarios. Therefore, one can conclude that the modeling framework employed in the LCA model provides a capacity hedging approach under uncertain demand with a stationary or non-stationary process. For further illustration, the example of the instance P6-HL-Con is reported in Figures B.8 and B.9 in Appendix B.

For the LAF model, Figure 7 shows that capacity follows demand for each typical scenario. This means that the scenario-dependent flows are adjusted to each scenario, and that the demand covered by the designed network is superposed with the demand scenario. This indicates that the LAF model converges to a solution driven by the expected value criterion, but does not anticipate any capacity hedging. It seems that LAF solutions are prone to greater efficiency in terms of capacity-allocation, but this comes at the price of no flexibility. Finally, to further underline is that in the 2E-DDP, the demand is covered with respect to the inbound allocation to DPs from warehouses, and not the DPs' predefined capacity. This is in accordance with the flow balance constraints at DPs, and emphasizes the impact of the two-echelon context considered in this work.

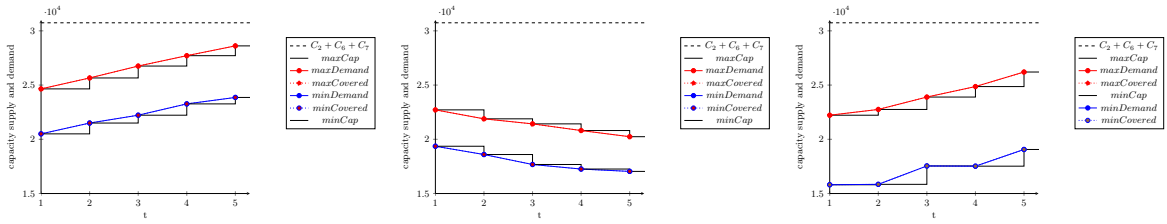

(a) NRT process (b) NDT process (c) CRT process

Figure 7: Capacity decisions versus demand for Dis-P6-LL-500 in (LAF(Ω^N))

7. Conclusion

In this paper, we introduce a comprehensive methodology for the stochastic multi-period two-echelon distribution network design problem (2E-DDP) where products are directed from primary warehouses to distribution platforms (DPs) before being transported to ship-to-points. The problem is characterized by a temporal hierarchy between the design level dealing with DP location decisions and capacity decisions, and the operational level involving transportation decisions as origin-destination flows. A stochastic multi-period scenario-based characterization of the planning horizon is considered, shaping the evolution of the uncertain ship-to-point demand. This problem is initially formulated as a multi-stage stochastic program, and we propose alternative two-stage multi-period modeling approaches to capture the essence of the problem, while providing judicious accuracy-solvability trade-offs. Consequently, the two models proposed are: the two-stage stochastic location and capacity-allocation model (LCA) in which DP location decisions and capacity decisions are first-stage decisions, and the two-stage stochastic flow-based location-allocation model (LAF) where capacity decisions are transformed into continuous scenario-dependent origin-destination links within the second-stage. To solve these models, we develop a Benders decomposition approach integrated with the sample average approximation (SAA) method. We also examine the value of the stochastic solution and compare it to the deterministic solution. Extensive computational experiments are run to validate the modeling and the solution approaches.

The computational experiments lead to several key findings. The findings underline the importance of integrating the strategic decisions when designing a two-echelon structure of a distribution network. In all the instances, the DPs location opening are driven by the inbound assignment-capacity from the primary warehouses, and not only by outbound operations. In addition, the results validate our proposed two-stage stochastic decisional models to capture the essence of the dynamic setting in the 2E-DDP. The LCA model tends to hedge against all scenarios which enhances its flexibility in terms of DPs opening and provides a dynamic management of capacity in time. The LAF model is scenario-driven and produces efficient solutions in terms of capacity-allocation, but this comes at the price of less flexibility in terms of DPs capability. Further, the computational experiments highlight the importance of modeling uncertainty on the 2E-DDP, and the limited quality of solutions produced by the deterministic formulation of the problem. Finally, the results show the limitation of basic commercial solvers and stochastic programming tools, such as SAA, to solve medium- and large-sized instances. As shown, these latter instances of the 2E-DDP necessitate the development of Benders approach to guarantee their resolution.

Although the Benders decomposition provides good-quality solutions, its performance is limited for large-scale instances in terms of solution time (more than 40 hours). It might be worthwhile improving the considered algorithm by introducing an initial good solution and an upper bound on the problem that are generated heuristically to reduce the runtime. In addition, adding Pareto-optimal cut helps to enhance its performance. Further, we believe that our framework provides ample opportunities for additional research. Future works could develop efficient heuristics to solve larger problem instances. Another interesting research direction could consider stochastic multi-period two-echelon distribution network design problems with more complex features where the location decisions of the two echelons (warehouses and DPs) are questioned, and where operational decisions are modeled by multi-drop routes, and/or multiple product families need to be distinguished. Additionally, it would be interesting to add financial risk measures to the objective function, such as mean semi-deviation and

conditional value at risk, or supply chain risk measures as discussed in [34]. Another extension of this work consists in tackling the multi-stage stochastic program, and further proposing performance measures on the quality of the obtained solutions compared to two-stage stochastic models. However, this remains a challenging task, given the curse of dimensionality of multi-stage problems.

Acknowledgements

The experiments presented in this paper were carried out using the PlaFRIM (Federative Platform for Research in Computer Science and Mathematics), created under the Inria PlaFRIM development action with support from Bordeaux INP, LABRI and IMB, and other entities: Conseil Régional d'Aquitaine, Université de Bordeaux, CNRS and ANR in accordance to the "Programme d'Investissements d'Avenir" (see www.plafrim.fr/en/home).

References

[1] Aghezzaf, E. (2005). Capacity planning and warehouse location in supply chains with uncertain demands. *Journal of the Operational Research Society*, *56*, 453–462.

[2] Ahmed, S., King, A. J., & Parija, G. (2003). A multi-stage stochastic integer programming approach for capacity expansion under uncertainty. *Journal of Global Optimization*, *26*, 3–24.

[3] Albareda-Sambola, M., Alonso-Ayuso, A., Escudero, L. F., Fernández, E., & Pizarro, C. (2013). Fix-and-relax-coordination for a multi-period location–allocation problem under uncertainty. *Computers & Operations Research*, *40*, 2878–2892.

[4] Albareda-Sambola, M., Fernández, E., & Nickel, S. (2012). Multiperiod location-routing with decoupled time scales. *European Journal of Operational Research*, *217*, 248–258.

[5] Ambrosino, D., & Scutellà, M. G. (2005). Distribution network design: new problems and related models. *European Journal of Operational Research*, *165*, 610–624.

[6] Badri, H., Bashiri, M., & Hejazi, T. H. (2013). Integrated strategic and tactical planning in a supply chain network design with a heuristic solution method. *Computers & Operations Research*, *40*, 1143–1154.

[7] Bashiri, M., Badri, H., & Talebi, J. (2012). A new approach to tactical and strategic planning in production–distribution networks. *Applied Mathematical Modelling*, *36*, 1703–1717.

[8] Beltran-Royo, C., Escudero, L. F., & Rodriguez-Ravines, R. E. (2010). Multi-stage stochastic linear programming: Scenarios versus events, .

[9] Benders, J. (2005). Partitioning procedures for solving mixed-variables programming problems. *Computational Management Science*, *2*, 3–19.

[10] Benders, J. F. (1962). Partitioning procedures for solving mixed-variables programming problems. *Numerische Mathematik*, *4*, 238–252.

[11] Birge, J. R., & Louveaux, F. (2011). *Introduction to stochastic programming*. Springer Science & Business Media.

[12] Boccia, M., Crainic, T., Sforza, A., & Sterle, C. (2011). *Location-routing models for two-echelon freight distribution system design*. Technical Report CIRRELT.

[13] Canel, C., Khumawala, B. M., Law, J., & Loh, A. (2001). An algorithm for the capacitated, multi-commodity multi-period facility location problem. *Computers & Operations Research*, *28*, 411–427.

[14] Consortium, T. S. C. (2011). Network design practices - how sophisticated is your supply chain network? http://archive.tompkinsinc.com/wp-content/uploads/2012/07/network-design-practices.pdf. Accessed: 2017-09-10.

[15] Contardo, C., Hemmelmayr, V., & Crainic, T. G. (2012). Lower and upper bounds for the two-echelon capacitated location-routing problem. *Computers & Operations Research*, *39*, 3185–3199.

[16] Correia, I., Melo, T., & da Gama, F. S. (2013). Comparing classical performance measures for a multi-period, two-echelon supply chain network design problem with sizing decisions. *Computers & Industrial Engineering*, *64*, 366–380.

[17] Cortinhal, M. J., & Melo, M. J. L. M. T. (2015). Dynamic design and re-design of multi-echelon, multi-product logistics networks with outsourcing opportunities: a computational study. *Computers & Industrial Engineering*, *90*, 118–131.

[18] Crainic, T. G., Ricciardi, N., & Storchi, G. (2004). Advanced freight transportation systems for congested urban areas. *Transportation Research Part C: Emerging Technologies*, *12*, 119–137.

[19] Cuda, R., Guastaroba, G., & Speranza, M. G. (2015). A survey on two-echelon routing problems. *Computers & Operations Research*, *55*, 185–199.

[20] Darvish, M., Archetti, C., Coelho, L. C., & Speranza, M. S. (2019). Flexible two-echelon location routing problem. *European Journal of Operational Research*, .

[21] Daskin, M. S. (1995). *Network and Discrete Location: Models, Algorithms and Applications*. Wiley-Interscience Publication, New York.

[22] Drexl, M., & Schneider, M. (2015). A survey of variants and extensions of the location-routing problem. *European Journal of Operational Research*, *241*, 283–308.

[23] Dunke, F., Heckmann, I., Nickel, S., & da Gama, F. S. (2018). Time traps in supply chains: Is optimal still good enough? *European Journal of Operational Research*, *264*, 813–829.

[24] Dupačová, J., Consigli, G., & Wallace, S. W. (2000). Scenarios for multistage stochastic programs. *Annals of operations research*, *100*, 25–53.

[25] Dupačová, J., Gröwe-Kuska, N., & Römisch, W. (2003). Scenario reduction in stochastic programming. *Mathematical Programming*, *95*, 493–511.

[26] Farahani, R. Z., Hekmatfar, M., Fahimnia, B., & Kazemzadeh, N. (2014). Hierarchical facility location problem: Models, classifications, techniques, and applications. *Computers & Industrial Engineering*, *68*, 104–117.

[27] Fattahi, M., Mahootchi, M., Govindan, K., & Husseini, S. M. M. (2015). Dynamic supply chain network design with capacity planning and multi-period pricing. *Transportation Research Part E: Logistics and Transportation Review*, *81*, 169–202.

[28] Geoffrion, A. M., & Graves, G. W. (1974). Multicommodity distribution system design by benders decomposition. *Management Science*, *20*, 822–844.

[29] Georgiadis, M. C., Tsiakis, P., Longinidis, P., & Sofioglou, M. K. (2011). Optimal design of supply chain networks under uncertain transient demand variations. *Omega*, *39*, 254–272.

[30] Gonzalez-Feliu, J. (2008). *Models and methods for the city logistics: The two-echelon capacitated vehicle routing problem*. Ph.D. thesis Politecnico di Torino.

[31] Graves, S. C. (1996). A multi-echelon inventory model with fixed replenishment intervals. *Management Science*, *42*, 1–18.

[32] Guan, Y., Ahmed, S., & Nemhauser, G. L. (2009). Cutting planes for multistage stochastic integer programs. *Operations Research*, *57*, 287–298.

[33] Hakimi, S. (1964). Optimum locations of switching centers and the absolute centers and medians of a graph. *Operations Research*, *12*, 450–459.

[34] Heckmann, I., Nickel, S., & da Gama, F. S. (2016). The risk-aware multi-period capacitated plant location problem (cplp-risk). In *International Conference on Information Systems in Supply Chain*.

[35] Heitsch, H., & Römisch, W. (2009). Scenario tree modeling for multistage stochastic programs. *Mathematical Programming*, *118*, 371–406.

[36] Hochreiter, R. (2016). Modeling multi-stage decision optimization problems. In *Computational Management Science* (pp. 209–214). Springer.

[37] Høyland, K., & Wallace, S. W. (2001). Generating scenario trees for multistage decision problems. *Management Science*, *47*, 295–307.

[38] Huang, K., & Ahmed, S. (2009). The value of multistage stochastic programming in capacity planning under uncertainty. *Operations Research*, *57*, 893–904.

[39] Jacobsen, S., & Madsen, O. (1980). A comparative study of heuristics for a two-level location-routing problem. *European Journal of Operational Research*, *6*, 378–387.

[40] Jena, S. D., Cordeau, J. F., & Gendron, B. (2015). Dynamic facility location with generalized modular capacities. *Transportation Science*, *49*, 484–499.

[41] Jones, C. (2018). Sam's club closing dozens of stores; some being converted to distribution centers. `https://eu.usatoday.com/story/money/2018/01/11/sams-club-closing-dozens-stores-reports-say/1024986001/`. Accessed: 2018-03-05.

[42] Kaut, M., Midthun, K., Werner, A., Tomasgard, A., Hellemo, L., & Fodstad, M. (2014). Multi-horizon stochastic programming. *Computational Management Science*, *11*, 179–193. doi:doi:10.1007/s10287-013-0182-6.

[43] Klibi, W., Lasalle, F., Martel, A., & Ichoua, S. (2010). The stochastic multiperiod location transportation problem. *Transportation Science*, *44*, 221–237.

[44] Klibi, W., & Martel, A. (2013). The design of robust value-creating supply chain networks. *OR Spectrum*, *35*, 867–903.

[45] Klibi, W., Martel, A., & Guitouni, A. (2016). The impact of operations anticipations on the quality of stochastic location-allocation models. *Omega*, *62*, 19–33.

[46] Laporte, G. (1988). Location-routing problems. In B. L. Golden, & A. A. Assad (Eds.), *Vehicle Routing: Methods and Studies* (pp. 163–198). North-Holland, Amsterdam.

[47] Maggioni, F., & Wallace, S. W. (2012). Analyzing the quality of the expected value solution in stochastic programming. *Annals of Operations Research*, *200*, 37–54.

[48] Martel, A., & Klibi, W. (2016). Supply chain networks optimization. In *Designing Value-Creating Supply Chain Networks* (pp. 243–287). Springer.

[49] Melo, M. T., Nickel, S., & da Gama, F. S. (2009). Facility location and supply chain management–a review. *European Journal of Operational Research*, *196*, 401–412.

[50] Nguyen, V. P., Prins, C., & Prodhon, C. (2012a). Solving the two-echelon location routing problem by a grasp reinforced by a learning process and path relinking. *European Journal of Operational Research*, *216*, 113–126.

[51] Nguyen, V. P., Prins, C., & Prodhon, C. (2012b). A multi-start iterated local search with tabu list and path relinking for the two-echelon location-routing problem. *Engineering Applications of Artificial Intelligence*, *25*, 56–71.

[52] Nickel, S., da Gama, F. S., & Ziegler, H. P. (2012). A multi-stage stochastic supply network design problem with financial decisions and risk management. *Omega*, *40*, 511–524.

[53] Pimentel, B. S., Mateus, G. R., & Almeida, F. A. (2013). Stochastic capacity planning and dynamic network design. *International Journal of Production Economics*, *145*, 139–149.

[54] Prodhon, C., & Prins, C. (2014). A survey of recent research on location-routing problems. *European Journal of Operational Research*, *238*, 1–17.

[55] Rockafellar, R. T., & Wets, R. J.-B. (1991). Scenarios and policy aggregation in optimization under uncertainty. *Mathematics of Operations Research*, *16*, 119–147.

[56] Römisch, W., & Schultz, R. (2001). Multistage stochastic integer programs: An introduction. In *Online Optimization of Large Scale Systems* (pp. 581–600). Springer.

[57] Santoso, T., Ahmed, S., Goetschalckx, M., & Shapiro, A. (2005). A stochastic programming approach for supply chain network design under uncertainty. *European Journal of Operational Research*, *167*, 96–115.

[58] Schültz, R. (2003). Stochastic programming with integer variables. *Mathematical Programming*, *97*, 285–309.

[59] Schütz, P., Tomasgard, A., & Ahmed, S. (2009). Supply chain design under uncertainty using sample average approximation and dual decomposition. *European Journal of Operational Research*, *199*, 409–419.

[60] Shapiro, A. (2003). Monte carlo sampling methods. *Handbooks in Operations Research and Management Science*, *10*, 353–425.

[61] Shapiro, A. (2008). Stochastic programming approach to optimization under uncertainty. *Mathematical Programming*, *112*, 183–220.

[62] Shapiro, A., Dentcheva, D., & Ruszczynski, A. (2009). *Lectures on stochastic programming: modeling and theory*. The Society for Industrial and Applied Mathematics and the Mathematical Programming Society, Philadelphia, USA.

[63] Skar, C., Doorman, G., Pérez-Valdés, G., & Tomasgard, A. (2016). *A multi-horizon stochastic programming model for the European power system*. Technical Report CenSES working paper.

[64] Slyke, R. M. V., & Wets, R. (1969). L-shaped linear programs with applications to optimal control and stochastic programming. *SIAM Journal on Applied Mathematics*, *17*, 638–663.

[65] Sterle, C. (2010). *Location-Routing models and methods for Freight Distribution and Infomobility in City Logistics*. Ph.D. thesis Università degli Studi di Napoli "Federico II".

[66] Verter, V., & Dincer, M. C. (1995). Facility location and capacity acquisition: an integrated approach. *Naval Research Logistics*, *42*, 1141–1160.

[67] Vila, D., Martel, A., & Beauregard, R. (2006). Designing logistics networks in divergent process industries: A methodology and its application to the lumber industry. *International Journal of Production Economics*, *102*, 358–378.

[68] Vila, D., Martel, A., & Beauregard, R. (2007). Taking market forces into account in the design of production-distribution networks: A positioning by anticipation approach. *Journal of Industrial and Management Optimization*, *3*, 29.

[69] Zeballos, L. J., Méndez, C. A., & Barbosa-Povoa, A. P. (2016). Design and planning of closed-loop supply chains: A risk-averse multistage stochastic approach. *Industrial & Engineering Chemistry Research*, *55*, 6236–6249.

[70] Zhuge, D., Yu, S., Zhen, L., & Wang, W. (2016). Multi-period distribution center location and scale decision in supply chain network. *Computers & Industrial Engineering*, *101*, 216–226.

Appendix A. Solution methodology

Appendix A.1. Sample Average Approximation (SAA)

Under a scenario-based optimization approach, building scenarios $\omega \in \Omega$ and assessing their probabilities $p(\omega)$ could entail a tremendous effort. Moreover, generating the adequate sample of scenarios $|\Omega|$, $\Omega = \cup_{t\in T}\Omega_t$, could be complex due to the large number of scenarios required under a high degree of uncertainty and the enumeration issue induced by continuous probability distributions [62]. The combination of the Monte Carlo sampling methods [60] and the SAA technique [62] helps in finding a good trade-off in terms of the scenarios' probability estimation and the sufficient number of scenarios to consider in the design model. The approach is to generate, outside the optimization procedure, an independent sample of N equiprobable scenarios $\{\omega^1, \ldots, \omega^N\} = \Omega_t^N \subset \Omega_t$ from the initial probability distribution, which also eliminates the need to explicitly compute the scenario probabilities $p(\omega)$. Then, the SAA program is built and the adequacy of the sample size validated by optimization. Hereafter, for instance, the SAA program related to the LCA model is provided, denoted with (LCA(Ω^N)):

$$(\mathrm{LCA}(\Omega^N)) \quad \mathcal{V}^N = \min \sum_{t\in\mathcal{T}}\sum_{l\in\mathcal{L}}(f_{lt}^u\, y_{lt} + f_{lt}^s\, z_{lt}) + \sum_{t\in\mathcal{T}}\sum_{l\in\mathcal{L}}\sum_{p\in\mathcal{P}} c_{lpt}\, C_{lp} x_{lpt} + \frac{1}{N}\sum_{t\in\mathcal{T}}\sum_{\omega\in\Omega_t^N}\sum_{j\in\mathcal{J}} d_{j\omega t}[\sum_{l\in\mathcal{L}} c_{ljt}\, v_{lj\omega t} + c_{j\omega t}\, s_{j\omega t}] \tag{A.1}$$

$$\text{S. t.} \quad (12) - (16)$$

$$\sum_j d_{j\omega t}\, v_{lj\omega t} \leqslant \sum_p C_{lp} x_{lpt} \qquad \forall l \in \mathcal{L}, t \in \mathcal{T}, \omega \in \Omega_t^N \tag{A.2}$$

$$\sum_l v_{jl\omega t} + s_{j\omega t} = 1 \qquad \forall j \in \mathcal{J}, t \in \mathcal{T}, \omega \in \Omega_t^N \tag{A.3}$$

$$v_{lj\omega t}, s_{j\omega t} \geqslant 0 \qquad \forall l \in \mathcal{L}, j \in \mathcal{J}, \omega \in \Omega_t^N, t \in \mathcal{T} \tag{A.4}$$

It is well established that the optimal value $\mathcal{V}^N(o)$ of the optimal design vector $\widehat{X}^N(o)$ of each SAA program $o \in \{\mathrm{LCA}(\Omega^N), \mathrm{LAF}(\Omega^N)\}$ converges to optimality as the sample size increases [62]. This suggests that the quality of the SAA models improves as the size of the sample employed grows. However, one would in practice choose N, taking into account the trade-off between the quality of the obtained design for each SAA program o and the computational effort needed to solve it ([45]). In such case, solving the SAA program with M independent samples repeatedly can be more insightful than increasing the sample size N. This leads to calculating a statistical optimality gap for each obtained design vector $\widehat{X}^N(o)$ by estimating the lower and upper bounds. The SAA-based procedure employed to calibrate the samples-size for both the LCA and LAF models is given in 3.

Worth noting is that the upper bound $\mathcal{V}^{N'}(\widehat{X}_m^N(o))$ proposed in step 4 for each model o is computed as follows: in the case of the (LCA(Ω^N)) model,

$$\mathcal{V}^{N'}(\hat{X}_m^N(\mathrm{LCA}(\Omega^N))) = \sum_{t\in\mathcal{T}}\sum_{l\in\mathcal{L}}(f_{lt}^u\, \hat{y}_{lt} + f_{lt}^s\, \hat{z}_{lt}) + \sum_{t\in\mathcal{T}}\sum_{l\in\mathcal{L}}\sum_{p\in\mathcal{P}} c_{lpt}\, C_{lp} \hat{x}_{lpt} + \frac{1}{N'}\sum_{t\in\mathcal{T}}\sum_{\omega\in\Omega_t^{N'}} Q_t(\hat{x}_m^N, \omega)$$

Algorithm 3 The SAA method to give model o

1: Generate M independent samples Ω_m^N, $m = 1, \ldots, M$ of N scenarios and solve the SAA program for each sample. Let $\mathcal{V}_m^N(o)$ and $\widehat{X}_m^N(o)$ be the corresponding optimal value and the optimal design solution, respectively.
2: Compute the statistical lower bound:

$$\bar{\mathcal{V}}_M^N(o) = \frac{1}{M} \sum_{m=1..M} \mathcal{V}_m^N(o)$$

3: Choose a feasible solution $\widehat{X}_m^N(o)$
4: Estimate the upper bound using a reference sample $N' \gg N$, $\mathcal{V}^{N'}(\widehat{X}_m^N(o))$
5: Compute an estimate of the statistical optimality gap of solution $\widehat{X}_m^N(o)$:

$$gap_M^{N,N'}(\widehat{X}_m^N(o)) = \mathcal{V}^{N'}(\widehat{X}_m^N(o)) - \bar{\mathcal{V}}_M^N(o)$$

An estimate of the average gap for the sample of size N is given by:

$$gap^{N,N'}(o) = \frac{1}{M} \sum_{m=1..M} gap_M^{N,N'}(\widehat{X}_m^N(o))$$

6: **if** *acceptable*(*gap*) **then**
7: **return** $gap^{N,N'}$
8: **else**
9: Repeat step 1-5 using larger N and/or M.
10: **end if**

and in the case of (LAF(Ω^N)),

$$\mathcal{V}^{N'}(\widehat{X}_m^N(\mathrm{LAF}(\Omega^N))) = \sum_{t\in\mathcal{T}} \sum_{l\in\mathcal{L}} (f_{lt}^u\, \hat{y}_{lt} + f_{lt}^s\, \hat{z}_{lt}) + \frac{1}{N'} \sum_{t\in\mathcal{T}} \sum_{\omega\in\Omega_t^{N'}} Q_t(\hat{y}_m^N, \omega)$$

Appendix A.2. The Benders reformulation for (LAF(Ω^N))

The primal sub-problem for each ω and t is:

$$(\mathrm{PS}_{\omega t}) \quad \phi_{t\omega}(y,z) = \min \sum_{l\in\mathcal{L}} \sum_{p\in\mathcal{P}} c_{lpt}\, C_{lp} x_{lpt\omega} + \sum_j d_{j\omega t} [\sum_l c_{ljt}\, v_{lj\omega t} + c_{j\omega t}\, s_{j\omega t}] \tag{A.5}$$

$$\text{S. t.} \quad \sum_{l\in\mathcal{L}} C_{lp} x_{lpt\omega} \leqslant C_p \qquad \forall p \in \mathcal{P} \tag{A.6}$$

$$\sum_{p\in\mathcal{P}} C_{lp} x_{lpt\omega} \leqslant C_l\, y_{lt} \qquad \forall l \in \mathcal{L} \tag{A.7}$$

$$\sum_j d_{j\omega t}\, v_{lj\omega t} - \sum_p C_{lp} x_{lpt\omega} \leqslant 0 \qquad \forall l \tag{A.8}$$

$$\sum_l v_{lj\omega t} + s_{j\omega t} = 1 \qquad \forall j \tag{A.9}$$

$$x_{lpt\omega} \geqslant 0 \qquad \forall l, p \tag{A.10}$$

$$v_{lj\omega t} \geqslant 0 \qquad \forall l, j \tag{A.11}$$

$$s_{j\omega t} \geqslant 0 \qquad \forall j \tag{A.12}$$

Its dual is :

$$(\mathrm{DS}_{\omega t}) \quad \phi_{t\omega}(y,z) = \max \sum_p C_p \theta_p + \sum_l C_l\, y_{lt}\, \gamma_l + \sum_j \beta_j \tag{A.13}$$

$$\text{S. t.} \quad C_{lp}\theta_p + C_{lp}\gamma_l - C_{lp}\alpha_l \leqslant c_{lpt} C_{lp} \qquad \forall l, p \tag{A.14}$$

$$d_{j\omega t}\, \alpha_l + \sum_j \beta_j \leqslant d_{j\omega t}\, c_{ljt} \qquad \forall l, j \tag{A.15}$$

$$\beta_j \leqslant d_{j\omega t}\, c_{j\omega t} \qquad \forall j \tag{A.16}$$

$$\theta_p \leqslant 0 \qquad \forall p \tag{A.17}$$

$$\gamma_l, \alpha_l \leqslant 0 \qquad \forall l \tag{A.18}$$

$$\beta_j \in \mathbb{R} \qquad \forall j \tag{A.19}$$

Then, the master problem is as follows:

$$\text{(MastP)}\min \sum_{lt}(f^u_{lt}\, y_{lt} + f^s_{lt}\, z_{lt}) + \frac{1}{N}\sum_{t\omega} u_{t\omega} \tag{A.20}$$

$$\text{S. t.} \quad (14) \text{ and } (16)$$

$$u_{t\omega} - \sum_l C_l\, y_{lt}\, \gamma_l \geqslant \sum_j \beta_j + \sum_p C_p\, \theta_p \qquad \forall t, \omega, (\theta_p, \gamma_l, \alpha_l, \beta_j) \in P_{\Delta_{t\omega}} \tag{A.21}$$

$$u_{tw} \geqslant 0 \qquad \forall t, \omega \tag{A.22}$$

Appendix A.3. The deterministic model (EV)

$$\text{(EV)}\min \sum_{l\in\mathcal{L}}\sum_{t\in\mathcal{T}}(f^u_{lt}\, y_{lt} + f^s_{lt}\, z_{lt}) + \sum_{l\in\mathcal{L}}\sum_{p\in\mathcal{P}}\sum_{t\in\mathcal{T}} c_{lpt}\, C_{lp} x_{lpt} + \sum_{t\in\mathcal{T}}\sum_{j\in\mathcal{J}} \mu_{jt}[\sum_{l\in\mathcal{L}} c_{ljt}\, v_{ljt} + c_{jt}\, s_{jt}] \tag{A.23}$$

$$\text{S. t.} \quad \sum_{l\in\mathcal{L}} C_{lp} x_{lpt} \leqslant C_p \qquad \forall p \in \mathcal{P}, t \in \mathcal{T} \tag{A.24}$$

$$\sum_{p\in\mathcal{P}} C_{lp} x_{lpt} \leqslant C_l\, y_{lt} \qquad \forall l \in \mathcal{L}, t \in \mathcal{T} \tag{A.25}$$

$$y_{lt} - y_{lt-1} \leqslant z_{lt} \qquad \forall l \in \mathcal{L}, t \in \mathcal{T} \tag{A.26}$$

$$\sum_j \mu_{jt}\, v_{ljt} \leqslant \sum_p C_{lp} x_{lpt} \qquad \forall l \in \mathcal{L}, t \in \mathcal{T} \tag{A.27}$$

$$\sum_l v_{jlt} + s_{jt} = 1 \qquad \forall j \in \mathcal{J}, t \in \mathcal{T} \tag{A.28}$$

$$x_{lpt} \in \mathbb{N} \qquad \forall l \in \mathcal{L}, p \in \mathcal{P}, t \in \mathcal{T} \tag{A.29}$$

$$y_{lt}, z_{lt} \in \{0, 1\} \qquad \forall l \in \mathcal{L}, t \in \mathcal{T} \tag{A.30}$$

$$v_{ljt} \geqslant 0 \qquad \forall l \in \mathcal{L}, j \in \mathcal{J}, t \in \mathcal{T} \tag{A.31}$$

$$s_{jt} \geqslant 0 \qquad \forall j \in \mathcal{J}, t \in \mathcal{T} \tag{A.32}$$

Appendix A.4. Quality of the stochastic solution

To characterize stochastic solutions, several indicators can be computed [11, 47]. The first is the statistical optimality gap estimate of the best solution identified by the SAA method for different sample sizes N as described in subsection Appendix A.1. Furthermore, the value of the stochastic solution (VSS), the loss using the skeleton solution (LUSS), and the loss of upgrading the deterministic solution (LUDS) proposed in [47] are also assessed as indicators of the quality of the stochastic solutions produced. Let $X^*(o)$ be the optimal solution obtained from the model $o \in \{\text{LCA, LAF}\}$, the here and now solution, under all $\omega \in \Omega$, and let RP be the optimal value of the associated objective function. More specifically, RP is computed by (A.33). Under a sampling approach, $\Omega^N \subset \Omega$, $\widehat{X}(o)$ represents the near-optimal solution obtained from the SAA program $o \in \{\text{LCA}(\Omega^N), \text{LAF}(\Omega^N)\}$. A good estimate of RP is given by (A.34).

$$RP = \mathbb{E}_\Omega[h(X^*(o), \Omega)] \tag{A.33}$$

$$\widehat{RP} = \mathcal{V}^N = \mathbb{E}_{\Omega^N}[h(\widehat{X}(o), \Omega^N)] \tag{A.34}$$

A common approach in the literature is to consider the expected value problem, where all the random variables are replaced by their expected value $\bar{\omega} = \mathbb{E}(\omega)$, solving the deterministic model (EV) as given in (A.35). Let $\bar{X}(o)$ be the optimal solution to (A.35), referred to as the expected value solution. The evaluation of its expected value (EEV) is computed as given in (A.36). Thus, the estimate of the value of the stochastic solution VSS is defined by formula (A.37), and measures the expected gain from solving a stochastic model rather than its deterministic counterpart.

$$EV = \min h(X(o), \bar{\omega}) \tag{A.35}$$

$$\widehat{EEV} = \mathbb{E}_{\Omega^N}[h(\bar{X}(o), \Omega^N)] \tag{A.36}$$

$$\widehat{VSS} = \widehat{EEV} - \widehat{RP} \tag{A.37}$$

The expected value solution $\bar{X}(o)$ may behave very badly in a stochastic environment. We here propose investigating how the expected value solution relates to its stochastic counterpart. For this purpose, we compute the loss using the skeleton solution (LUSS) and the loss of upgrading the deterministic solution (LUDS), which provide deeper information than the VSS on the structure of the problem [47]. To calculate the LUSS, we fix at zero all first-stage variables, which are at zero in the expected value solution $\bar{X}(o)$, and solve the SAA stochastic program $o \in \{\text{LCA}(\Omega^N), \text{LAF}(\Omega^N)\}$ with these additional constraints. Considering the program (LCA(Ω^N)), the additional constraints are:

$$x_{lpt} = 0 \qquad \forall l, p, t \in \mathcal{K}(\bar{x}, 0) \tag{A.38}$$

$$y_{lt} = 0 \qquad \forall l, t \in \mathcal{K}(\bar{y}, 0) \tag{A.39}$$

$$z_{lt} = 0 \qquad \forall l, t \in \mathcal{K}(\bar{z}, 0) \tag{A.40}$$

where $\mathcal{K}(\bar{x}, 0)$, $\mathcal{K}(\bar{y}, 0)$ and $\mathcal{K}(\bar{z}, 0)$ are sets of indices for which the components of the expected value solution $\bar{X} = \{\bar{x}, \bar{y}, \bar{z}\}$ are at zero. In the (LAF(Ω^N)), only constraints (A.39)-(A.40) are added. The solution of this program gives the near-optimal solution $\check{X}(o)$. Thus, an estimate of the expected skeleton solution value (ESSV) is computed with (A.41). Comparing it to the $\widehat{RP}$ estimate leads to an estimate of the LUSS as computed in (A.42). This test allows investigating why a deterministic solution may behave badly. In the case of $\widehat{LUSS} = 0$, this corresponds to the perfect skeleton solution in which the stochastic solution takes the deterministic solution values. Otherwise, in case of $0 < \widehat{LUSS} \leqslant \widehat{VSS}$, it means that alternative decision variables are chosen for the expected solution, thus providing alternative solution values.

$$\widehat{ESSV} = \mathbb{E}_{\Omega^N}[h(\check{X}(o), \Omega^N)] \tag{A.41}$$

$$\widehat{LUSS} = \widehat{ESSV} - \widehat{RP} \tag{A.42}$$

The last indicator considers the expected value solution $\bar{X}(o)$ as a starting point (input) to the stochastic program $o \in \{\text{LCA}(\Omega^N), \text{LAF}(\Omega^N)\}$, and compares, in terms of objective functions, the same program without such input. This helps test whether the expected value solution $\bar{X}(o)$ is upgradeable to become good (if not optimal) in the stochastic setting. To do so, one needs to solve the program o with additional constraints that ensure the expected value solution $\bar{X}(o)$ as a starting solution, thus obtaining the solution $\tilde{X}(o)$. More specifically, for the (LCA(Ω^N)) program, additional constraints are:

$$x_{lpt} \geqslant \bar{x}_{lpt} \qquad \forall l, p, t \tag{A.43}$$

$$y_{lt} \geqslant \bar{y}_{lt} \qquad \forall l, t \tag{A.44}$$

$$z_{lt} \geqslant \bar{z}_{lt} \qquad \forall l, t \tag{A.45}$$

However, the (LAF(Ω^N)) program considers only constraints (A.44)-(A.45). The expected input value is then computed with with (A.41), and this value is used to provide an estimate of the LUDS with formula (A.41). Worth noting is that $\widehat{LUDS} = 0$ corresponds to perfect upgradability of the deterministic solution, whereas $0 < \widehat{LUDS} \leqslant \widehat{VSS}$ leads to no upgradability.

$$\widehat{EIV} = \mathbb{E}_{\Omega^N}[h(\tilde{X}(o), \Omega^N)] \tag{A.46}$$

$$\widehat{LUDS} = \widehat{EIV} - \widehat{RP} \tag{A.47}$$

Appendix B. Results

Table B.11: Average statistical optimality gap values

		$gap^{N,2000}$ (%)				
		LCA(Ω^N)			**LAF**(Ω^N)	
Sample size N		100	200	500	200	500
Instance	P1-NRT-LL-N$\bar{s}$	0.26	0.26	0.21	0.01	-0.01
	P1-NDT-LL-N$\bar{s}$	0.03	0.01	-0.01	**0**	-0.02
	P1-CRT-LL-N$\bar{s}$	0.80	0.31	0.07	-0.05	-0.02
	P2-NRT-LL-N$\bar{s}$	0.61	0.23	0.08	0.06	**0**
	P2-NDT-LL-N$\bar{s}$	0.28	0.12	-0.01	**0**	-0.02
	P2-CRT-LL-N$\bar{s}$	0.60	0.24	0.06	-0.04	-0.02
	P3-NRT-LL-N$\bar{s}$			0.17		0.01
	P3-NDT-LL-N$\bar{s}$			-0.04		-0.04
	P3-CRT-LL-N$\bar{s}$			0.1		-0.02
	P4-NRT-LL-N$\bar{s}$	0.22	0.09	0.05	0.02	0.02
	P4-NDT-LL-N$\bar{s}$	0.15	0.01	0.01	**0**	0.01
	P4-CRT-LL-N$\bar{s}$	0.97	0.42	0.28	-0.04	-0.04

Table B.12: Mean value and MSD deviations for (LCA(Ω^N)) for problem sizes P4 and P5

		P4-LL-500						**P5-LL-500**					
		NDT		**NRT**		**CRT**		**NDT**		**NRT**		**CRT**	
		% $\mathcal{V}^e$	% MSD	% $\mathcal{V}^e$	% MSD	% $\mathcal{V}^e$	% MSD	% $\mathcal{V}^e$	% MSD	% $\mathcal{V}^e$	% MSD	% $\mathcal{V}^e$	% MSD
Dis-	s1	**0**	**0**	**0**	**0**	0.14	42.15	0.34	67.77	0.03	**0**	0.02	15.18
	s2	**0**	**0**	**0**	**0**	**0**	**0**	0.01	1.27	**0**	9.16	0.02	8.30
	s3	**0**	**0**	**0**	**0**	0.14	42.15	0.05	31.11	**0**	9.16	**0**	**0**
	s4	**0**	**0**	**0**	**0**	1.20	78.42	0.07	30.91	0.03	0.05	0.02	15.18
	s5	**0**	**0**	**0**	**0**	**0**	**0**	**0**	12.45	**0**	9.16	0.02	15.18
	s6	**0**	**0**	**0**	**0**	0.14	42.15	**0**	**0**	**0**	9.05	0.02	15.18
Con-	s1	**0**	**0**	**0**	1.29	**0**	1.42	0.04	10.07	0.08	**0**	0.01	12.36
	s2	**0**	**0**	**0**	1.29	0.09	**0**	**0**	**0**	0.08	**0**	0.06	9.40
	s3	**0**	**0**	**0**	1.29	**0**	1.42	0.04	10.07	**0**	42.32	**0**	**0**
	s4	**0**	**0**	0.11	**0**	**0**	1.42	0.04	10.07	**0**	42.32	0.01	12.36
	s5	**0**	**0**	**0**	1.29	0.21	14.22	0.04	10.07	0.08	**0**	**0**	**0**
	s6	**0**	**0**	**0**	1.29	0.12	15.63	0.04	10.07	0.08	**0**	0.01	12.36

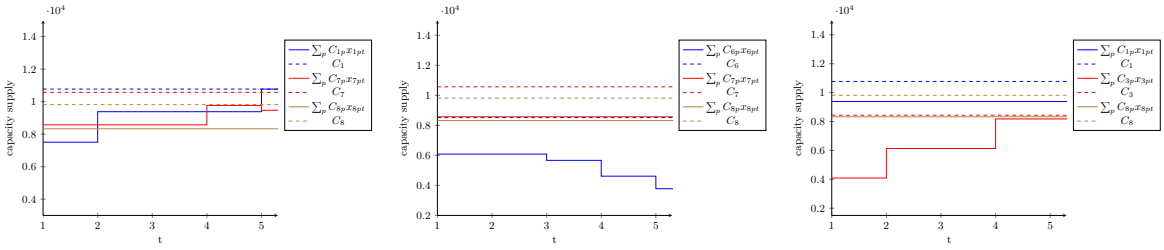

(a) NRT process (b) NDT process (c) CRT process

Figure B.8: Capacity allocation decisions versus the a priori capacity for Con-P6-HL-500 in (LCA(Ω^N))

Table B.13: Mean value and MSD deviations for (LCA(Ω^N)) for problem sizes P2 and P3

		P2-LL-500						**P3-LL-500**					
		NDT		**NRT**		**CRT**		**NDT**		**NRT**		**CRT**	
		% $\mathcal{V}^e$	% MSD	% $\mathcal{V}^e$	% MSD	% $\mathcal{V}^e$	% MSD	% $\mathcal{V}^e$	% MSD	% $\mathcal{V}^e$	% MSD	% $\mathcal{V}^e$	% MSD
Dis-	s1	**0**	4.71	0.07	3.74	0.28	**0**	**0**	1.09	0.15	7.62	0.48	29.32
	s2	0.05	**0**	0.02	1.38	0.03	3.39	**0**	1.09	0.03	**0**	**0**	1.47
	s3	0.13	14.77	**0**	**0**	**0**	4.56	**0**	1.09	0.01	10.19	0.01	**0**
	s4	0.01	3.61	0.02	1.38	0.04	6.70	0.04	**0**	0.01	12.06	0.01	**0**
	s5	0.04	9.18	**0**	**0**	0.12	2.31	**0**	1.09	**0**	2.77	0.01	**0**
	s6	0.06	7.01	0.09	3.26	0.09	2.56	**0**	1.09	0.22	20.56	0.01	**0**
Con-	s1	0.02	2.84	**0**	**0**	0.03	3.56	**0**	**0**	**0**	12.11	**0**	**0**
	s2	**0**	**0**	**0**	**0**	0.06	5.28	**0**	**0**	**0**	12.11	0.16	12.68
	s3	**0**	0.07	0.06	20.49	0.06	5.28	**0**	**0**	0.08	**0**	0.21	7.83
	s4	0.03	4.08	**0**	**0**	0.01	1.55	**0**	**0**	**0**	12.11	**0**	**0**
	s5	0.01	1.91	**0**	**0**	**0**	**0**	**0**	**0**	0.08	**0**	**0**	**0**
	s6	**0**	0.67	**0**	**0**	0.04	6.02	**0**	**0**	0.08	**0**	**0**	**0**

Table B.14: Best location decisions for (LCA(Ω^N))

	Dispersed ship-to-points (Dis)																							
	NRT-500								**NDT-500**								**CRT-500**							
DPs	**l1**	**l2**	**l3**	**l4**	**l5**	**l6**	**l7**	**l8**	**l1**	**l2**	**l3**	**l4**	**l5**	**l6**	**l7**	**l8**	**l1**	**l2**	**l3**	**l4**	**l5**	**l6**	**l7**	**l8**
P1-LL	1		1						1		1						1		1					
P1-HL	1		1						1		1						1		1					
P2-LL		1				1		1		1				1		1		1				1		1
P2-HL		1				1		1		1				1		1		1				1		1
P3-LL		2			1	1				2	1					1		2	2					1
P3-HL	1				1	1				2	1					1		2	2					1
Concentric ship-to-points (Con)																								
P1-LL	1			1					1			1					1			1				
P1-HL	1			1					1			1					1			1				
P2-LL	1		1			1		1	1		1			1		1	1		1			1		1
P2-HL	1		1			1		1	1		1					1	1		1					1
P3-LL	2		1			1		1	2		1			2			2		1					1
P3-HL	2		2					1	1		1			2			1		1					1

1 and 2 refer to the Capacity configuration

Table B.15: Best location decisions for (LAF(Ω^N))

	Dispersed ship-to-points (Dis)																							
	NRT-500								**NDT-500**								**CRT-500**							
DPs	**l1**	**l2**	**l3**	**l4**	**l5**	**l6**	**l7**	**l8**	**l1**	**l2**	**l3**	**l4**	**l5**	**l6**	**l7**	**l8**	**l1**	**l2**	**l3**	**l4**	**l5**	**l6**	**l7**	**l8**
P1-LL	1		1						1		1						1		1					
P1-HL	1		1						1		1						1		1					
P2-LL		1				1		1		1				1		1		1				1		1
P2-HL		1				1		1		1				1		1		1				1		1
P3-LL		1	1					1		1	1					1		1	1					1
P3-HL		1	1					1						2		2		1	1					1
Concentric ship-to-points (Con)																								
P1-LL	1			1					1			1					1			1				
P1-HL	1			1					1			1					1			1				
P2-LL	1		1					1	1		1			1			1		1					1
P2-HL	1		1					1	1		1			1			1		1					1
P3-LL	2		1					1	1		1			1			1		1					1
P3-HL	2		1					1	1		1			1			1		1					1

1 and 2 refer to the Capacity configuration

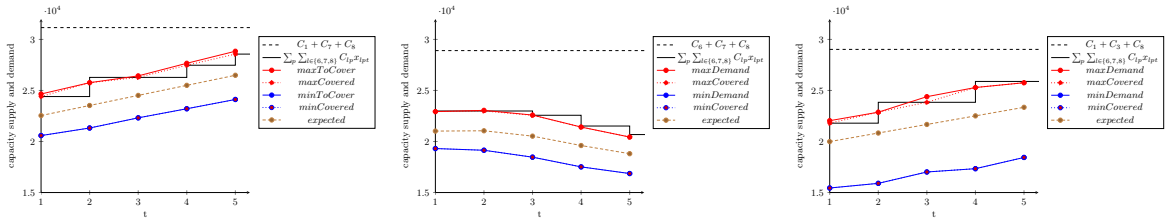

(a) NRT process (b) NDT process (c) CRT process

Figure B.9: Capacity decisions versus demand for Con-P6-HL-500 in (LCA(Ω^N))

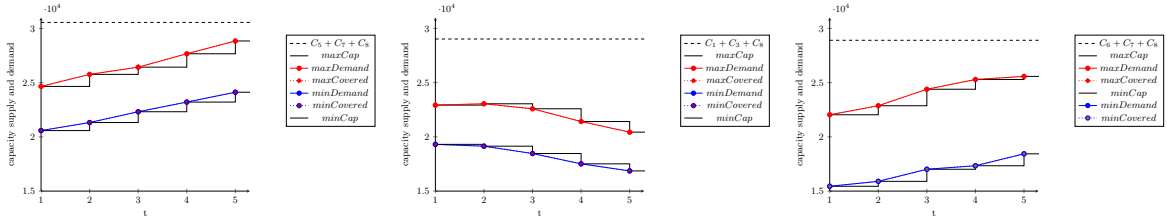

(a) NRT process (b) NDT process (c) CRT process

Figure B.10: Capacity decisions versus demand for Con-P6-HL-500 in (LAF(Ω^N))